THE UNIVERSITY OF CHICAGO

CONSERVED PATTERNS OF FUNCTIONAL ORGANIZATION BETWEEN CORTEX AND THALAMUS IN MICE

A DISSERTATION SUBMITTED TO

THE FACULTY OF THE DIVISION OF THE BIOLOGICAL SCIENCES

AND THE PRITZKER SCHOOL OF MEDICINE

IN CANDIDACY FOR THE DEGREE OF

DOCTOR OF PHILOSOPHY

COMMITTEE ON NEUROBIOLOGY

BY

ANDREW J. MILLER

CHICAGO, ILLINOIS

JUNE 2022

"The new apparatus seemed to be misbehaving very badly indeed, and I suddenly found it was behaving so well that it was opening up an entire new range of data. . . . it didn't involve any particular hard work, or any particular intelligence on my part. It was just one of those things which sometimes happens in a laboratory if you stick apparatus together and see what results you get."

-Edgar Douglas Adrian

TABLE OF CONTENTS

LIST OF FIGURES

LIST OF TABLES

LIST OF ABBREVIATIONS

AP5, (2R)-amino-5-phosphonovaleric acid; **ChR2**, channelrhodopsin; **dLGN**, dorsal lateral geniculate nucleus; **DNQX**: 6,7-dinitroquinoxaline-2,3-dione; **EPSC/P**, excitatory postsynaptic current/potential; **FO**, first-order; **HO**, higher-order; **HVA**, higher visual area; **iGluR**, ionotropic glutamate receptor; **M1**, primary motor cortex; **MGBv**, ventral Medial geniculate nucleus; **mGluR**, metabotropic glutamate receptor; **NMDA**, N-methyl-D-aspartate; **POm**, posterior medial nucleus; **PPR**, paired-pulse ratio; **PrV**, principal trigeminal nucleus; **Pul**, pulvinar; **S1**, primary somatosensory cortex; **S2**, secondary somatosensory cortex; **SC**, superior colliculus; **SpV**, spinal trigeminal nucleus; **V1**, primary visual cortex; **VPm**, ventral posterior medial nucleus.

ACKNOWLEDGEMENTS

This work and my graduate education wouldn't have been possible without my partner, Dr. Grace T. Hansen, with whom I have so much fun that long and difficult days still feel too short. I've never met someone with so much energy, and the fraction that rubs off on me makes all the difference sometimes.

Thank you to my parents and siblings for teaching me to believe in education and encouraging curiosity. I'd also like to thank the peers, committee members, and other mentors who have inspired and encouraged me to spend a great deal of time and energy on learning new things. My main advisor as an undergraduate, Dr. Eric Norstrom, told me that, "you're not born knowing how to do everything," and he was right.

The Sherman Lab has been a great place to spend graduate school. Thanks to my lab mates, some of whom are close friends who I look forward to seeing progress as scientists. I've learned a great deal from all of them, especially Dr. Sherman. Murray has been a supportive mentor and great role model from whom I'll be borrowing phrases and ideas for as long as I'm a scientist.

Lastly, I'd like to acknowledge that there's something different about the scientists who devote themselves to the study of the brain. To me, understanding how physical material gives rise to our thoughts, feelings, and humanity is the most interesting question we can hope to address. Thanks to all of you for your work. Much of this dissertation concerns the anatomy and physiology of the thalamus, including the pulvinar. In ancient Rome, a "pulvinar" was a cushion or empty throne, sometimes a place for votive offerings, awaiting occupation by a deity. Perhaps in the brain there is an inhabitant, a Ghost or an ego that operates the machinery, but I think it's a more likely and more beautiful possibility that the brain operates itself. And at the center, there is simply an empty throne.

ABSTRACT

Higher-order thalamic nuclei contribute to sensory processing via projections to primary and higher cerebral cortical areas, but it is unknown which of their cortical and subcortical inputs contribute to their distinct output pathways. We used sub-population specific viral strategies in mice to anatomically and physiologically dissect pathways of the higher order thalamic nuclei of the somatosensory and visual systems (the posterior medial nucleus and pulvinar).

Employing a complementary optogenetics and electrical stimulation strategy, we show that synapses in cortex from higher order thalamus have functionally divergent properties in primary vs. higher cortical areas. Higher order thalamic projections onto excitatory targets in S1 and V1 were weakly modulatory while projections to S2 and higher visual areas were strong drivers of postsynaptic targets.

Then, using transsynaptic tracing verified by optogenetics to map inputs to higher order thalamus, we show that posterior medial nucleus cells projecting to S1 are driven by neurons in layer 5 of S1, S2, and M1, and that pulvinar cells projecting to V1 are driven by neurons in layer 5 of V1 and higher visual areas. Therefore, in both systems, layer 5 of primary and higher cortical areas drives transthalamic feedback modulation of primary sensory cortex through higher order thalamus.

These results highlight conserved organization that may be shared by other thalamocortical circuitry. They also support the hypothesis that direct corticocortical projections in the brain are paralleled by transthalamic pathways, even in the feedback direction, with feedforward transthalamic pathways acting as drivers, while feedback through thalamus is modulatory.

CHAPTER 1: GENERAL INTRODUCTION

1.1 The Inner Room

The thalamus (from the Greek *thalamos* or, "inner room,") is a mass of cell bodies and fibers roughly in the center of the brain, densely interconnected with many other regions, especially those of the cerebral cortex. The cells of the thalamus are divided into nuclei, mostly in a mosaic fashion rather than by discrete borders, and these nuclei associate with cortex according to many different anatomical patterns of inputs and outputs. As a sort of crossroads, the thalamus is ideally situated to act as a hub of activity in several brain systems. While the complex and diverse connections of the thalamus have always made its study a challenge, the dedicated work of anatomists and physiologists have given us a great deal of information from which to draw conclusions. In this project, we have leveraged that literature along with modern techniques of molecular biology and electrophysiology to describe several common organizational features of the thalamocortical systems mediating somatosensation and vision in the mouse. While much of this project describes many small details of the circuitry underlying sensory perception, we will also discuss how, along with the work of many others as described below, these details can help us to see conserved patterns of thalamocortical interactions across sensory systems. Lastly, we will describe how these conserved patterns can point us to generalizable principles of information flow between cortical areas and help us to understand how patterns of neuronal activity can represent the external world.

1.2 The Thalamus in Sensory Perception

In the early nineteenth century, it was already understood that damage to the thalamus generally led to sensory deficits (E. G. Jones, 2007), and this insight led to the modern textbook view of the thalamus as a, "sensory relay," or, "sensory switchboard" (Sherman & Guillery, 2013). This incomplete view of the thalamus was based on early studies of first-order (FO) sensory

thalamic nuclei, those nuclei that receive strong input from sub-cortical sources conveying sensory information from the periphery, and relay that information to primary sensory cortical areas (e.g. retina → dLGN → V1 in the visual system and PrV → VPM → S1 in the somatosensory system). In these pathways, receptive field information is conveyed to thalamic relay cells, which in turn project mainly to layer 4 of primary sensory cortical areas, delivering the main source of sensory input to cortex, which then processes that information further enabling the coordinated cortical activity thought to underlie sensory perception (more on this below in 1.3). For example, pharmacological or optogenetic silencing of the dLGN in awake rats nearly abolishes the activity in V1 (Murata & Colonnese, 2016)(Reinhold et al., 2015). The inputs and outputs of FO thalamic nuclei such as dLGN, VPM, and MGBv are relatively well studied, and while certainly important for sensory function, in fact make up the minority by volume of the thalamus of rodents, cats, and primates (Sherman & Guillery, 2013).

The majority of the thalamus is composed of higher-order (HO) thalamic nuclei, which receive strong input from layer 5 of cortex, sometimes in combination with sub-cortical inputs, and relay that activity back to several cortical areas (Figure 1.1). Nuclei of the HO thalamus are poorly understood, either in terms of the complex patterns of connections individual cells make or in terms of the nature of the messages being transmitted by HO thalamus to targets in cortex. HO thalamic nuclei include the pulvinar in the visual system (from the latin *pulvinus* or, "cushion," here abbreviated Pul, also sometimes called LP in rodents), the posteriomedial nucleus (POm) in the somatosensory system, and the dorsal medial geniculate body (MGBd) in the auditory system. As shown in Figure 1.1, HO thalamus sends projections to both primary sensory cortical areas, as well as higher cortical areas (this hierarchical relationship between cortical areas will be described further, below in 1.3). However, until recently, it remained a mystery which of the many inputs to

HO thalamic nuclei fed into its distinct output pathways, or to what degree the different projections from HO thalamus arise from the same individual cells with branching axons vs. separate cell populations. This project and other recent findings have begun to unravel the organization of these nuclei, as discussed in chapters 2 and 3.

Figure 1.1: A Schematic of FO and HO Thalamocortical Circuits

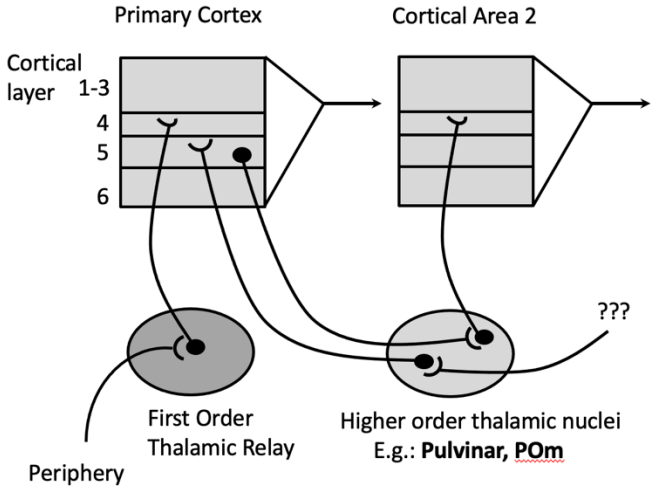

FO thalamic nuclei receive sensory input from sub-cortical sources and send robust projections to layer 4 of primary sensory cortical areas. HO thalamic nuclei receive strong input from layer 5 of cortex and send projections to various cortical areas at different points along the cortical hierarchy. Individual cells in HO thalamic nuclei receive inputs from different cortical areas, sometimes in combination with sub-cortical inputs. Therefore, it is possible that projection-defined sub-populations in HO thalamus may receive different input patterns, and therefore relay different messages to their cortical targets. Feedforward transthalamic pathways sending activity from a lower cortical area to a higher one have been described in the somatosensory and visual systems, but it is not known what inputs drive the HO thalamic projections to primary sensory cortical areas.

In general, the sensory-evoked activity of HO thalamus is modest, and neural activity in POm and Pul strongly correlates with movement and arousal state (Petty et al., 2021). Similarly, lesions in the HO visual nucleus Pul not only cause simple sensory deficits but rather can cause spatial neglect (Rafal & Posner, 1987) and impaired attention (Snow et al., 2009). It has also been shown that while passive detection of a whisker stimulus in rats does not strongly engage the HO nucleus POm, active sensing (i.e. requiring the animal to move its whiskers to feel the shape of something) does engage POm (Pais-Vieira et al., 2013), again supporting the notion that HO thalamic nuclei

play a role in sensorimotor integration and perhaps in representing the relevant behavioral context of a sensory stimulus.

1.3 The Cortex in Sensory Perception

The recently evolved neocortex, a sheet of six layers of cells forming the outer shell of the cerebrum, and referred to here for simplicity as, "cortex," represents sensory stimuli through the coordinated activation of ensembles of cells, and does so reliably, despite high trial to trial variability in the responses of individual cortical cells (L. M. Jones et al., 2007; Shadlen & Newsome, 1994). These representations can change over time or with training (Yang & Maunsell, 2004), and therefore must be both robust and flexible. The ways cortical circuitry accomplishes this feat are not the focus of this project, but to appreciate the ways that thalamic inputs to cortex contribute to sensory perception and sensorimotor integration, we will briefly describe the hierarchical organization of cortex and the flow of sensory-evoked signals in the brain.

The textbook view of cortical processing (reviewed in ((Callaway, 2004) and ((Hirsch & Martinez, 2006) begins with FO thalamus sending strong inputs to layer 4 of primary sensory cortical areas (such as V1 or S1). Post-synaptic responses in layer 4 are the least variable compared to other layers (Brumberg et al., 1999)(Brecht et al., 2003), and are thought to faithfully represent simple stimulus features, such as a particular contrast change, organized topographically across cortex. Within one cortical column, cells respond to related stimulus features, and each stage of cortical processing is thought to perform a distinct function on that signal (Martinez et al., 2005)(Hirsch & Martinez, 2006). Layer 4 cells project in turn to layers 2/3 at which point already responses become more variable, but also cells respond with larger receptive fields to more complex features of stimuli (Brumberg et al., 1999)(Martinez et al., 2005). The cells of layers 2/3

project to layer 5, and layer 5 sends strong projections down to HO thalamus, as well as to other subcortical motor centers (although some cells of layers 2/3 and 5 project horizontally to other cortical regions). Layer 5 also activates layer 6 of cortex, which sends modulatory feedback to FO and HO thalamus (described further below, in 1.4). In addition to these communications between layers within one cortical column, the cells of layers 2/3 also send feedforward projections to layer 4 of other cortical areas considered hierarchically secondary (Van Essen & Maunsell, 1983) (although in some cases feedforward projections also originate in deep layers, and indeed the overall laminar organization of output cells is not so strict in rodents (Sherman & Guillery, 2013)). These inputs then contribute to the further elaboration of receptive fields and representation of increasingly rich and complex stimulus features as information is processed in this cortical area and propagated further forward to higher cortical areas.

Feedback projections to regions hierarchically lower also shape cortical representations, with feedback in primates terminating outside of layer 4 (Van Essen & Maunsell, 1983). Feedforward projections are considered more topographically organized, and well-suited to conveying receptive field information up the sensory hierarchy, while feedback is often referred to as modulatory, due to its looser relationship to receptive field properties and diffuse anatomical organization (i.e. the presynaptic feedback axon may represent a specific stimulus feature, but it may also terminate over a large area synapsing onto cells responding to a wide range of stimuli) (Callaway, 2004). Regarding synaptic properties and the relative connection strength of feedforward and feedback connections in cortex, some data from within a single cortical column of mice support the notion that less-precisely organized feedback (such as from layer 6 to layer 4) indeed show synaptic properties suggestive of a modulatory role (Lee & Sherman, 2009), limited data from long-range projections between cortical areas complicate this picture. Slice physiology performed by our lab

showed that projections between V1 and V2 as well as between A1 and A2 also in mice were shown to be a mixture of strong "driving" and weak "modulatory" connections in both directions (De Pasquale & Sherman, 2011)(Covic & Sherman, 2011). Perhaps this is another distinction between rodents and primates, or it could be the case that connection strength is not so strictly divergent in the feedforward and feedback directions of corticocortical communications as previously thought.

1.4 Interactions between Cortex and Thalamus

The classic model of thalamus as a "sensory relay" indicates that FO thalamic inputs to layer 4 of primary sensory areas deliver the necessary sensory-evoked messages to cortex, which then amplifies and processes that input up cortical hierarchies without further need for thalamic involvement. However, this view ignores the vast diversity of thalamocortical connections, and it has been critiqued and improved over the years due to several lines of evidence showing that this view is vastly oversimplified. Most prominently, the contributions of HO thalamus to cortical function have begun to be appreciated. For example, a recent study in the somatosensory system of rats confirmed that the sensory-evoked response to whisker deflections in layers 2/3 of S1 cortex is comprised of an initial, fast, short-latency depolarization followed by hundreds of milliseconds of persistent activity (Zhang & Bruno, 2019). While the initial depolarization was dependent on the FO thalamic nucleus VPM, it could have been the case that the persistent activity was dependent solely on recurrent activity of intracortical circuitry, or alternatively that feedback input from higher cortical or thalamic areas was needed as well. Indeed, it was shown that only the silencing of HO thalamic nucleus POm affected the persistent activity, essentially abolishing it with short latency, and showing that HO thalamus is required for stable maintenance of neural

representations of sensory stimuli over hundreds of milliseconds. The work presented here (Chapter 2), will provide one possible explanation for this slower POm-dependent change in excitability, namely group I metabotropic glutamate receptors (mGluRs) present at POm → S1 synapses, which operate over a similar time-window. Similarly in the visual system of mice, it has been shown that optogenetic silencing of visual thalamus (both the FO dLGN and HO Pul) abolished the later phases of sensory-evoked visual cortical responses, even after allowing the initial stimulus-evoked response (Reinhold et al., 2015).

With regards to the cortical inputs to thalamus, an important functional distinction has been drawn between layer 5 and layer 6 of cortex, based on the anatomy and physiology of those corticothalamic synapses. While both form excitatory glutamatergic synapses, their functional divergence provides a good example of the utility of the "driver / modulator" framework for classifying glutamatergic synapses (reviewed in (Sherman & Guillery, 2013). Layer 5 corticothalamic terminals are a good example of a glutamatergic driver synapse: They form large synaptic terminals proximally located on the cells of HO thalamus, which evoke fast excitatory post-synaptic potentials (EPSPs), via ionotropic glutamate receptors only (largely AMPA and NMDA), exhibit paired-pulse depression (a characteristic of synapses with a high probability of neurotransmitter release which then diminishes as readily available neurotransmitter vesicles are depleted), and thus are generally well-suited to driving the post-synaptic cell to firing an action potential in a temporally-precise short time window. As expected, layer 5 cells and HO thalamic cells have a tightly-related cross-correlogram (i.e. HO thalamic cells fire shortly after layer 5 cells fire)(Sherman & Guillery, 2013), and the silencing of cortex, causes HO thalamic cells to also fall silent (Bender, 1983)(Diamond et al., 1992). On the other hand, corticothalamic projections from layer 6 show the reverse of all of these properties: they form small, distally located synapses on

both FO and HO thalamic relay cells, they evoke smaller and slower EPSPs via ionotropic and mGluRs, exhibit paired-pulse facilitation (a characteristic of synapses with a low initial probability of release, which facilitate in response to repetitive stimulation due to buildup of pre-synaptic calcium), and are therefore referred to as glutamatergic, "modulators," because they are well-suited to modulating the way the post-synaptic cell responds to other driver inputs. In keeping with this interpretation, silencing layer 6 input to the dLGN has little effect on response or receptive field properties (Richard et al., 1975). Worthy of noting is that while glutamatergic modulators affect post-synaptic targets in much the same way as some classical neuromodulators (e.g. acetylcholine, serotonin, etc.), as glutamatergic projections, they are often still topographically organized, whereas classical neuromodulators are diffusely organized. Therefore glutamatergic modulators are synapses which can exert modulatory influence, often based on cortical rather than brainstem signals, onto post-synaptic targets in a topographically organized fashion.

In the context of the hierarchical relationship between sensory cortical areas and the driver / modulator synapse distinction, we can revisit Figure 1, to describe the aims of this project. Figure 1 shows two separate projections from HO thalamus engaging cortex very differently. The HO thalamic cell furthest to the right receives its driving input from layer 5 of primary sensory cortex and relays that activity in the feedforward direction to layer 4 of secondary sensory cortex via another strong, driver-type projection. Such a pathway is referred to as a feedforward transthalamic pathway, emphasizing that it traverses HO thalamus in parallel to a direct cortico-cortical projection. This arrangement has been described in the somatosensory and visual systems ((Blot et al., 2021), (Theyel et al., 2010)), and while it is not yet clear why the brain sends both a direct and transthalamic pathway in a pattern of seemingly redundant wiring, it has been shown that these transthalamic pathways can strongly drive post-synaptic activity in the higher visual area LM and

in S2 ((Blot et al., 2021), (Theyel et al., 2010)). However, HO thalamus also projects to primary sensory cortex in both systems, but it is not known to what degree layer 5 of different cortical areas (or indeed sub-cortical inputs to thalamus) drives input to primary areas S1 and V1. This project, therefore, will leverage the well-studied mouse somatosensory and visual systems and recent advances in virally-mediated anatomy and neurophysiology methods explore the synaptic properties of HO thalamic projections to primary vs. higher cortical areas in the mouse somatosensory and visual systems with particular emphasis on criteria relevant to the driver / modulator distinction for classifying glutamate synapses, will then explore the anatomical inputs to HO thalamic cells projecting to primary areas to understand which of the many inputs to HO thalamus target or avoid cells projecting to primary sensory cortex, will confirm which of those inputs are likely to drive the activity being delivered to primary sensory cortex, and lastly will compare across sensory systems for patterns of thalamocortical functional organization that may generalize across brain systems.

CHAPTER 2: CONSERVED PATTERNS OF FUNCTIONAL ORGANIZATION BETWEEN CORTEX AND THALAMUS IN MICE

2.1: Significance Statement

Neuroanatomical tracing provides just a partial picture of information flow in the brain, because excitatory synapses are not all equal. Some strongly drive postsynaptic targets to transfer information, whereas others serve to modulate their responsiveness rather than mainly provide a conduit for information transfer. Here, we show conserved patterns of synaptic function across somatosensory and visual thalamocortical circuits in mice involving higher order thalamic nuclei with respect to these different sorts of synaptic action. These nuclei serve as hubs in transthalamic or cortico-thalamo-cortical pathways. We report that feedforward transthalamic circuits in the somatosensory and visual systems operate to efficiently transmit information, whereas feedback transthalamic circuits act to modulate their target areas. These patterns may generalize to other brain systems and show how methods of synapse physiology and molecular biology can inform the exploration of brain circuitry and information processing.

2.2: Introduction

Higher order (HO) thalamic nuclei and their contributions to sensory processes remain poorly understood both in terms of the information they transmit to cerebral cortex and the effects they exert on specific cortical targets. While first-order (FO) thalamic nuclei receive driving input from subcortical sources only and act as feedforward relays, HO thalamic nuclei may receive mixed driving inputs from the cortex and brainstem. Thus, the heterogeneous organization and diverse connectivity that make the HO thalamus a challenge to study are the same qualities that make it a computationally rich hub of brain activity. In turn, cells of HO thalamus project to

primary sensory cortex and higher cortical areas, suggesting that some of these pathways may be feedforward and some feedback, partly depending on whether they transmit information from subcortical or cortical sources.

Converging lines of evidence suggest that HO thalamic nuclei play an active role in early sensory processing in rodents and primates (Sherman, 2016)(Nakajima & Halassa, 2017)(Saalmann & Kastner, 2015)(Sherman & Guillery, 2013)(Sherman & Usrey, 2021). Damage to the HO visual thalamic nucleus, the pulvinar (Pul, also sometimes called the lateral posterior nucleus in mice and rats) in humans and non-human primates has been associated with a range of visual and attentional deficits(Rafal & Posner, 1987)·(Ward et al., 2002)·(Snow et al., 2009). Inactivation of Pul in primates or cats alters V1 responses to visual stimuli(de Souza et al., 2020)·(Purushothaman et al., 2012), and the activity of Pul axons in V1 of mice can be used to predict motor actions and visuomotor discrepancies(Roth et al., 2016). The Pul has also been shown to regulate attentional selection in primates and enable functional transmission of information from one cortical area to another(Saalmann et al., 2012)·(Purushothaman et al., 2012).

Similarly, the HO somatosensory thalamic nucleus, the posterior medial nucleus (POm), has been shown to exert strong effects on S1 responses to whisker stimulation(Zhang & Bruno, 2019)·(Mease et al., 2016), and it has been suggested that POm integrates incoming bottom-up input from the spinal trigeminal nucleus (SpV) with descending cortical inputs(Groh et al., 2014). A potential role for POm in integrating motor and sensory cues has been proposed(Hooks, 2017)·(Urbain et al., 2015)·(Mo & Sherman, 2019), and it also regulates interactions between cortical areas(Theyel et al., 2010)·(Sampathkumar, Miller-Hansen, Sherman, et al., 2021), generating another parallel between POm and Pul and lending support to the notion that HO thalamic nuclei play a role in interpreting sensory cues in behavioral contexts(Sherman & Guillery,

2013). However, a more detailed appreciation of the underlying circuitry is required to understand the specific ways in which HO thalamus contributes to cortical processing.

We directly compared input and output features of the HO somatosensory nucleus, POm, with those of the HO visual nucleus, Pul to clarify which aspects of functional organization are specific to each system or alternatively conserved across both. We asked two major questions of these HO pathways. The first question is: What effects do HO thalamocortical terminals exert on excitatory neurons at different levels of the cortical hierarchy? In particular, do POm and Pul drive or modulate targets in cortex, and does this depend on hierarchical level? It has been recently shown that silencing Pul in cats results in different effects on sensory responses at different points of the visual cortical hierarchy(de Souza et al., 2020). What differences in the synapse physiology at each target site might underlie this finding? The driver vs. modulator framework for classifying glutamatergic synapses using anatomical and physiological criteria has proven useful for parsing glutamatergic projections that can exert very different types of functional influence over postsynaptic targets (reviewed in refs.(Sherman, 2016)·(Bickford, 2016)). To apply the driver/modulator framework to HO thalamocortical projections in the visual and somatosensory systems of mice, we developed an optogenetics protocol in an *in vitro* slice preparation consistent with similar approaches using electrical stimulation(Viaene et al., 2011a)·(Viaene et al., 2011b). We then evaluated physiological and pharmacological characteristics of HO thalamocortical synapses onto excitatory neurons in different layers of primary and secondary somatosensory cortex (S1 and S2) as well as in primary and higher visual areas (V1 and HVAs). The somatosensory and visual systems both exhibited a similar divergence of synaptic properties between primary and higher cortical areas, wherein HO thalamus modulated S1 and V1 while strongly driving S2 and HVAs.

The second question is: Of the diverse cortical and subcortical inputs to HO thalamic cells, where does the activity relayed by HO thalamus to primary sensory cortex originate? We focused on the inputs to the POm → S1 and Pul → V1 pathways, because in both systems, evidence suggests that HO thalamic input to secondary areas are driven by layer 5 of primary sensory cortex in feedforward transthalamic pathways(Theyel et al., 2010),(Blot et al., 2021), possibly in combination with sub-cortical inputs(El-Boustani et al., 2020),(Kirchgessner et al., 2021). However, it is not known to what extent HO thalamic cells projecting to S1 or V1 carry signals from primary or higher sensory cortex, motor areas, sub-cortical sources, or a mixture. We addressed these questions using output-defined anatomical tracing in combination with optogenetic circuit mapping to reveal further similarities in the organization of the two systems.

These data reveal a previously undescribed form of transthalamic feedback from higher cortical areas, running parallel to corticocortical feedback projections, similar to transthalamic pathways connecting cortical areas in the feedforward direction. They also suggest that, whereas feedforward transthalamic projections appear to drive postsynaptic targets, feedback transthalamic projections modulate targets earlier in the cortical hierarchy. We find that these results in combination with other recent findings contribute novel insights into HO thalamocortical organization and information processing in sensory systems.

2.3: Results

2.3.1: HO thalamocortical projections differentially affect primary versus higher cortical areas

We first developed an optogenetic stimulation approach to characterize HO thalamocortical physiology in acute slices, validated by comparison with previous approaches using electrical stimulation (see fig. 1 and ref.(Viaene et al., 2011a)) and employing a slice preparation in which much of the connectivity between thalamus and cortex is preserved (Agmon

& Connors, 1991). We confirm previous findings regarding the POm projection to S1 (Viaene et al., 2011a) and extend them by recording postsynaptic responses to POm stimulation from cells in layers 2-6 of S2. Furthermore, since a connected slice preparation is not readily available in the visual system due to the geometry of thalamocortical projections in the adult mouse (but see ref.(MacLean et al., 2006)), we extended the above observation to the visual system by using optogenetics to stimulate axons arising from Pul while recording from cells in layers 2-6 of V1 and HVAs (largely area LM, but also areas AM and AL, see Table S1 and Discussion).

An important synaptic variable we measured was paired-pulse ratio (PPR), either depression or facilitation. However, several virally-mediated optogenetics protocols appear to affect PPRs when terminals are directly photostimulated(Jackman et al., 2014)·(Mo & Sherman, 2019). We thus adopted a strategy for measuring PPRs by photostimulating afferents via their axons >300 μm from the recorded cell and terminals, which ameliorated this problem (see below).

Thalamocortical synaptic properties for POm projections to S1 and S2. Expressing ChR2-Venus by AAV injection in POm (while avoiding the neighboring FO nucleus VPm, see Fig. 1a) led to characteristic laminar distributions of labeled axons and terminals in S1 (most dense in layer 5a) and S2 (most dense in layer 4 (Fig. 1b). In mice with such expression, we made acute slices and established whole cell recordings of putatively excitatory neurons in layers 2-6. In voltage clamp mode, excitatory postsynaptic currents (EPSCs) were recorded from many of these cells while applying 10Hz focal laser stimulation through the microscope objective to measure the PPR. As noted above, laser stimulation targeted ChR2-expressing axons >300μm from the recording site, recruiting the axons' action potential transmission without optically activating the terminals directly. In keeping with previous data, all POm synapses in S1 showed paired-pulse facilitation (i.e., the amplitude of the second evoked EPSC being larger than that of the first, leading to a PPR

> 1) with a mean PPR of 1.27 ± 0.07 (mean ± S.E.M. throughout; n = 12 cells; see Fig. 1e, 1i, Table S1). By comparison, POm synapses in S2 evoked paired-pulse depression (i.e., the second EPSC amplitude being smaller than that of the first, leading to a PPR < 1) with a mean PPR of 0.64 ± 0.05 (n = 13 cells; see Table S1). Thus, recorded PPRs were significantly different in S1 vs. S2 when considering only cells in layers 2/3 ($p = 6.7x10^{-4}$, Mann Whitney U test throughout unless otherwise specified) or pooling across all layers ($p = 3.9x10^{-7}$). All responses in cortex to 10Hz stimulation were blocked by bath application of ionotropic glutamate receptor (iGluR) antagonists DNQX and AP5 and had short latencies (3.51ms ± 0.14) consistent with previous measurements of monosynaptic responses to axonal stimulation of thalamocortical afferents(Mo & Sherman, 2019). As discussed further below, recordings in S2 focused on layers 2/3, but paired-pulse depression was observed in all layers (see Table S1). Initial EPSC amplitudes evoked were smaller for cells in S1 (12.0pA ± 1.60, n=12 cells) than for those in S2 (37.8pA ± 7.24) ($p = 1.3x10^{-3}$ for cells in layers 2/3 only, $p = 3.4x10^{-4}$ when pooling across all layers) (Fig. 1e, 1i), despite no significant difference in input resistances across areas (183MΩ ± 17.4 in S1 vs. 166MΩ ± 9.44 in S2, consistent with previous recordings in adult mice(Mo & Sherman, 2019)).

We also verify the observation that the stimulation of ChR2 terminals directly (rather than remotely stimulating the axons) results in an artificial synaptic depression in some pathways. In particular, the facilitating responses observed here with axonal activation became depressing when focal stimulation was delivered over the terminals and postsynaptic cell body (Fig. S1a). With axonal stimulation >300 μm from the recorded cell, we always measured facilitation in S1 and depression in S2. In depressing pathways (e.g., when recording in S2 or recordings below), terminal stimulation did not produce depression that significantly differed from that seen with axonal stimulation.

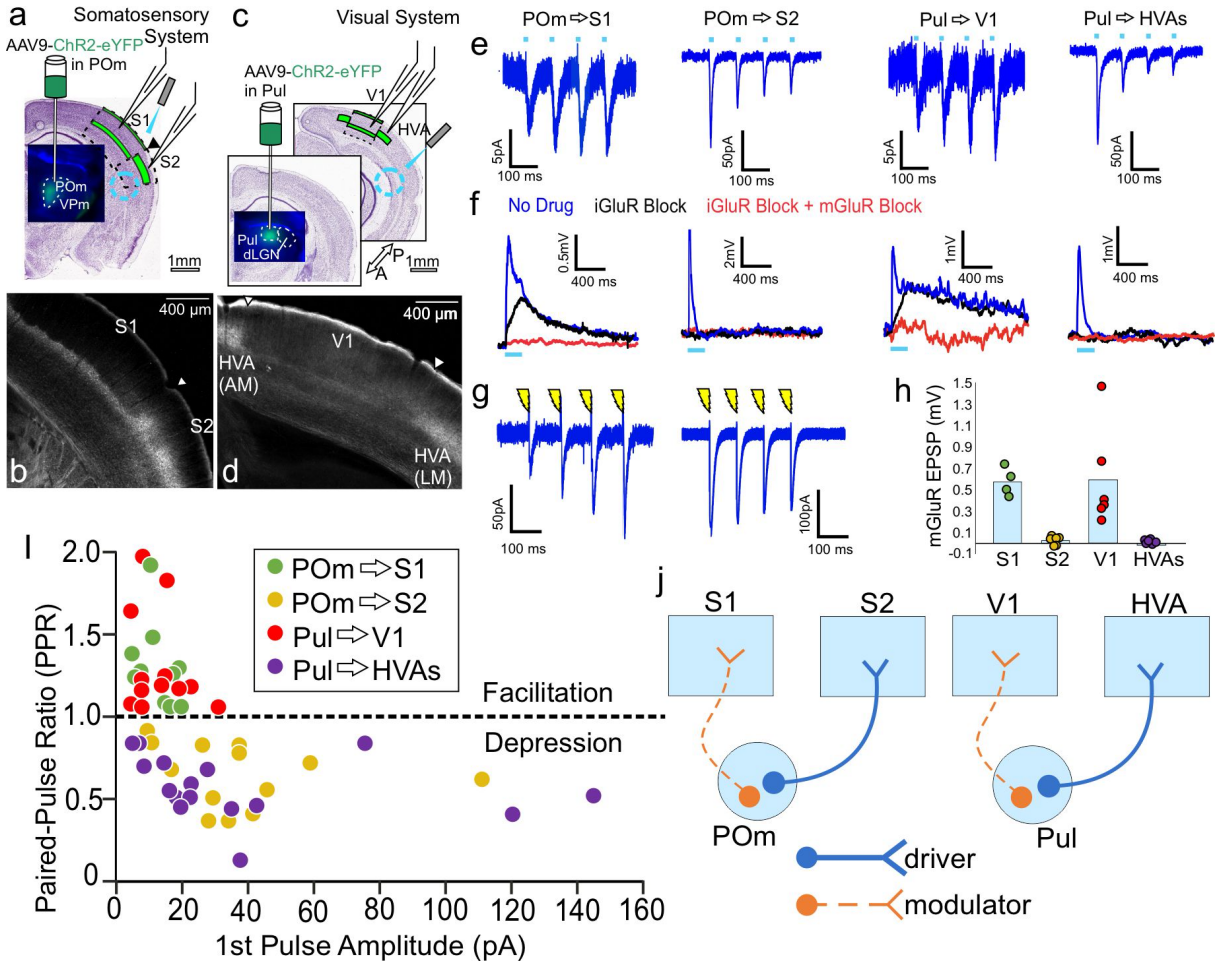

Figure 2.1. HO thalamocortical synapses exert different effects on primary vs. higher cortical areas.

(a) A schematic of experimental strategy to evaluate HO thalamocortical synapses in the somatosensory system. AAV9-pACAGW-ChR2-Venus was injected into the HO thalamic nucleus POm, allowing visualization and focal laser stimulation of POm axons in an acute slice during whole cell recordings from S1 or S2.

(b) ChR2-Venus + POm axons densely innervate layer 5a of S1 and layers 2/3 and 4 of S2, showing a clear border.

(c) Same experimental strategy as in (a), but evaluating HO thalamocortical synapses of the visual system by injecting AAV9-pACAGW-ChR2-Venus into Pul, allowing visualization and focal laser stimulation of Pul axons during whole cell recordings from V1 or HVAs.

(d) ChR2-Venus + Pul axons densely innervate layer 5a of V1 and layers 2/3 and 4 of HVAs, showing a clear border.

(e) Example voltage clamp recordings from S1 and S2 during optogenetic stimulation of POm axons (10Hz, 1ms pulse duration, >300µm away from the recording site), or from V1 or HVAs during. Stimulation of Pul axons. All 10Hz responses blockable with iGluR blockers DNQX and APV.

(f) Example current clamp recordings during high frequency stimulation over presynaptic terminals (83Hz, 1ms pulse duration) of the same HO thalamic axons as in I. Blue traces are responses before the application of drugs. Black traces are during bath application of iGluR blockers DNQX and APV, and red traces are in the presence of iGluR blockers and group 1 mGluR blockers LY367385 and MPEP.

(g) Example voltage clamp recordings from S1 and S2 during electrical stimulation of POm axons (10Hz, 0.1ms duration) in a connected thalamocortical slice.

Figure 2.1 continued

(h) mGluR-dependent responses to high frequency stimulation in S1 (n=4 cells), S2 (n=6), V1 (n=6), and HVAs (n=6). mGluR responses in S1 (0.58mV ± 0.07) and S2 (0.03mV ± 0.02) are significantly different from each other ($p = 9.5x10^{-3}$, Mann-Whitney U test throughout unless otherwise specified), and mGluR responses in V1 (0.59mV ± 0.19) and HVAs (-0.015mV ± 0.028) are significantly different from each other ($p = 2.2x10^{-3}$). Here and later figures, bars represent the mean while dots represent the data for individual cells.

(i) Scatterplot showing relationship of paired-pulse ratio (2^{nd} EPSC amplitude / 1^{st} EPSC amplitude) and amplitude of the 1^{st} evoked EPSC in a train for thalamocortical inputs to cortical neuronsData include cells in S1 (n=12, green), S2 (n=13, tan), V1 (n=12, red), and HVAs (n=16, purple). PPRs in S1 (1.27 ± 0.07, mean ± SEM throughout) and S2 (0.64 ± 0.05) are significantly different from each other ($p = 3.9x10^{-7}$), and PPRs in V1 (1.30 ± 0.09) and HVAs (0.57 ± 0.05) are significantly different from each other ($p = 6.6x10^{-8}$). Response amplitudes in S1 (12.0pA ± 1.60) and S2 (37.8pA ± 7.24) are significantly different from each other ($p = 3.4x10^{-4}$), and response amplitudes in V1 (13.3pA ± 2.35) and HVAs (38.8pA ± 10.21) are significantly different from each other ($p = 2.0x10^{-2}$).

(j) Summary of data interpreted in the context of glutamatergic *drivers* and *modulators.*

In current clamp mode, high frequency optogenetic stimulation (83Hz) was delivered over presynaptic terminals on a subset of cells to test for the activation of a slow metabotropic glutamate receptor (mGluR) dependent excitatory postsynaptic potentials (EPSPs) (Fig. 1f). High frequency stimulation evoked slow EPSPs in S1 recordings (mean amplitude 0.58mV ± 0.07, n = 4 cells), which could be blocked by group I mGluR antagonists (LY367385 and MPEP) and were dependent on repetitive stimulation(Viaene et al., 2013) (Fig.S1b). mGluR dependent EPSPs were absent in all recordings in S2 (0.03mV ± 0.02, n = 6 cells, $p = 9.5x10^{-3}$; Fig. 1h).

Therefore, properties of synapse physiology and pharmacology with known functional implications diverged notably for POm synapses in S1 vs. S2, consistent with their characterization as glutamatergic modulators and drivers, respectively (Fig. 1j, left).

Thalamocortical synaptic properties for Pul projections to V1 and HVAs. We then applied the same experimental approaches to the visual system. We expressed ChR2-Venus by AAV injection limited to Pul while avoiding delivering ChR2-Venus to neighboring structures, especially the lateral geniculate nucleus (dLGN) (Fig. 1c). As with the POm thalamocortical projections, Pul axons densely innervate layer 5a of V1 and layer 4 of HVAs (Fig. 1d). Again,

putatively excitatory cells were targeted for whole cell recordings. For all cells recorded in layers 2-6 in V1, responses to 10Hz stimulation of ChR2-axons >300um from the recorded cells evoked facilitating responses, with a mean PPR of 1.30 ± 0.09 (n = 12 cells; see Table S1), while those recorded in layers 2-6 of HVAs always evoked depressing responses (mean PPR 0.57 ± 0.05 n= 16 cells; Fig. 1e, 1i). PPRs were significantly different in V1 than HVAs when comparing cells in layers 2/3 ($p= 1.6x10^{-3}$) or when pooling across all layers ($p = 6.6x10^{-8}$). Also, initial EPSC amplitudes were smaller in V1 cells (13.3pA ± 2.35) compared with those in HVAs (38.8pA ± 10.21, $p = 2.0x10^{-2}$ pooling across all layers; Fig. 1e, 1i) despite no significant difference in input resistances across areas (194MΩ ± 20.2 for V1 vs. 176MΩ ± 14.5 for HVAs) and were blocked by bath application of iGluR antagonists. Finally, in a subset of cells, high frequency stimulation over presynaptic terminals evoked slow mGluR-dependent EPSPs in recordings in V1 (mean amplitude 0.59mV ± 0.19, n = 6) but not in HVAs (-0.015mV ± 0.028, n = 6, $p = 2.2x10^{-3}$; Fig 1f, 1h).

Overall, the visual system showed the same pattern as the somatosensory system, with properties of synapse physiology and pharmacology differing substantially between Pul synapses in V1 vs. HVAs, consistent with the hypothesis that Pul synapses in V1 act as glutamatergic modulators while those in HVAs act as drivers (Fig. 1j).

2.3.2: POm and Pul cells projecting to primary sensory cortex are innervated by layer 5 cells from multiple cortical areas.

Since thalamocortical projections from the POm and Pul evoke different postsynaptic responses at different points on the sensory cortical hierarchy, we asked: What are the driving inputs to POm and Pul cells projecting to these different cortical targets? Evidence suggests that HO thalamic input to secondary areas in both systems is driven by layer 5 of primary sensory

cortex forming feedforward transthalamic pathways (Theyel et al., 2010)·(Blot et al., 2021)·(Mo & Sherman, 2019), possibly integrated with sub-cortical inputs (El-Boustani et al., 2020)·(Kirchgessner et al., 2021). We therefore wanted to identify the driving inputs to POm and Pul cells projecting to primary sensory cortices. We first used an anatomical tracing technique to identify putative inputs to POm → S1 and Pul → V1 cells. We used an output-defined G-deleted rabies tracing strategy(Schwarz et al., 2015)·(Callaway & Luo, 2015), which retrogradely and trans-synaptically labels inputs to a particular sub-population of cells as defined by projection identity (see METHODS for details).

Identifying inputs to the POm → S1 pathway. By delivering cre to the POm → S1 population (via injection of AAVretro-cre or CAV-cre in S1), as well as cre-dependent rabies machinery (via AAV-FLEX-TVA-mCherry and AAV-G injection in POm), we rendered the POm → S1 population receptive to subsequent pseudo-typed rabies infection (i.e., RV-GFP), causing them to be double-labelled with mCherry and GFP. Only the double-labeled POm → S1 "starter cells" had the necessary receptor to accept rabies virus infection, and also had the rabies glycoprotein (G) necessary to transsynaptically label their presynaptic inputs (Fig. 2a). After validating that double-labeled "starter cells" were only present in POm (and not the neighboring FO ventral posterior medial nucleus, VPm, Fig. 2b) we searched for distant GFP-labeled presynaptic "input cells."

Due to well-known difficulties with leaky expression of TVA-mCherry and potential for false positives and negatives using this approach(Callaway & Luo, 2015), we developed a protocol with limited viral volumes to generate sparse labeling. We then did as follows: we manually screened each brain section; we discarded data from any animals with starter cells in the neighboring FO thalamic nucleus projecting to the same sensory cortical areas; we carefully

assessed controls lacking cre recombinase (Fig. S2d-f and 3d-f); and we validated key findings using optogenetics-based methods (below). Even with care taken to ensure the quality of anatomical data from G-deleted-rabies experiments, there are still many cell-type biases inherent to viral tracing techniques. Therefore, we regard these results as qualitatively informative regarding which areas project to the targeted POm → S1 and Pul → V1 sub-populations, and indeed they guided our optogenetics experiments described below, but they are not reliable for providing quantitative comparisons of input areas.

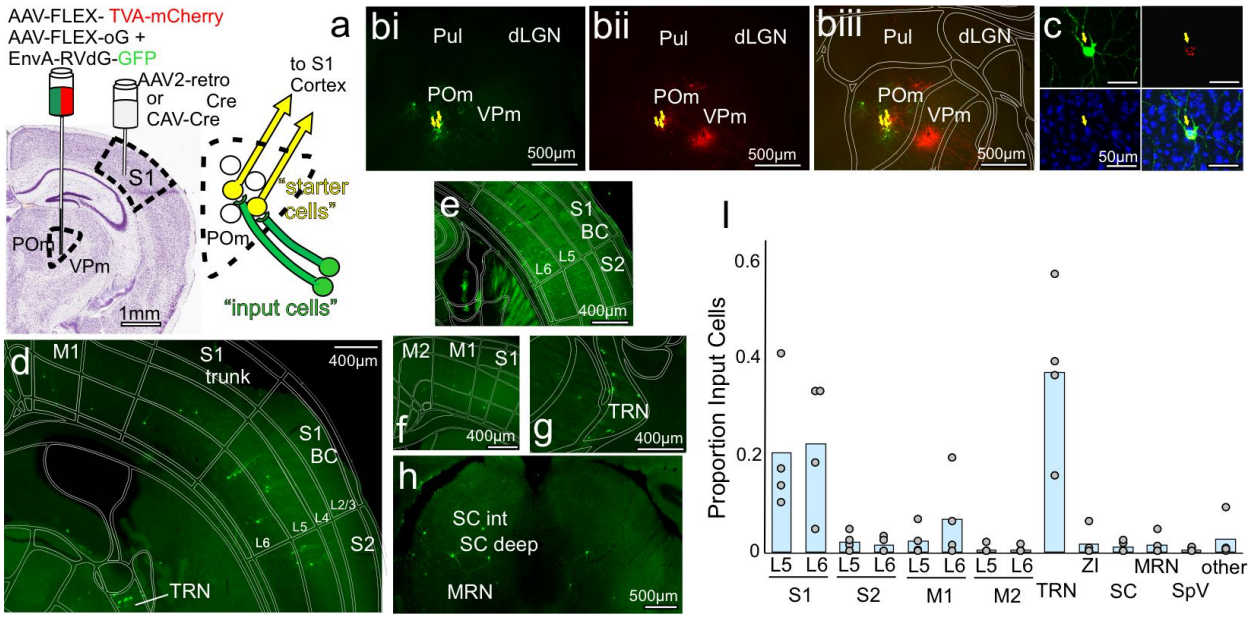

Figure 2.2: Retrograde transsynaptic tracing of inputs to the POm → S1 pathway

(a) Schematic of the anatomical labeling strategy for labeling presynaptic inputs to the POm → S1 pathway (see RESULTS and METHODS for details)
(b) Representative images of POm, with GFP+ (Bi) and mCherry+ (Bii) "starter" cells double labeled (yellow arrows) in POm only (overlay in Biii).
(c) Higher magnification image of a double labeled "starter" cell in POm, top left GFP, top right mCherry, bottom left DAPI, bottom right overlay.
(d-h) Representative epifluorescence images of GFP+ presynaptic "input" cells, projecting to the POm → S1 pathway. Cortical layers are labeled L2/3, L4, etc. Abbreviations: BC, Barrel cortex S1, TRN, thalamic reticular nucleus; SC int, SC intermediate layers; MRN, midbrain reticular nucleus.
(i) Location of presynaptic GFP+ input cells as a proportion of the number of input cells found in each mouse (n = 4 animals).

Inhibitory inputs from thalamic reticular nucleus (Fig. 2g) and zona incerta were labeled, as well as the layer 6 feedback corticothalamic cells (Fig. 2d,e,f) known to exert modulatory rather than driving input to thalamocortical cells(Sherman & Guillery, 2013)·(Kirchgessner et al., 2021)·(Reichova & Sherman, 2004). Among expected inputs, negligible label was seen in the spinal trigeminal nucleus (SpV) (2 cells in 2 animals, and no label in 2 animals)(Fig. 2i), which is known to relay whisker-related signals to POm(Veinante et al., 2000)·(Mo et al., 2017).

Prominent contributions of input to the POm → S1 pathway were found in layer 5 cells of S1 itself (Fig. 2d,e) as well as in layer 5 of S2 (Fig. 2d) and M1 (Fig. 2f); other inputs were also seen scattered in other areas (Fig. 2i). Because the layer 5 input to thalamus has been shown in many studies to be a strong, driving input (below, and refs.(Sherman & Guillery, 2013)·(Kirchgessner et al., 2021)·(Reichova & Sherman, 2004)), we used these anatomical results to direct further experiments testing whether the layer 5 cells identified by this transsynaptic tracing approach (those in S1, S2, and M1) indeed drive POm cells projecting to S1. We also explored the surprising lack of inputs from SpV (see below).

Identifying inputs to the Pul → V1 pathway. We next performed the analogous anatomical experiment aimed to identify inputs to Pul → V1 cells (Fig. 3a). We limited cre expression to the Pul → V1 sub-population by delivering it via a retrograde viral injection in V1, then cre-dependent rabies machinery tagged with mCherry was delivered to the Pul, followed by RV-GFP, leaving double-labeled Pul → V1 "starter cells" (Fig. 3b), and distant GFP-only presynaptic "input cells."

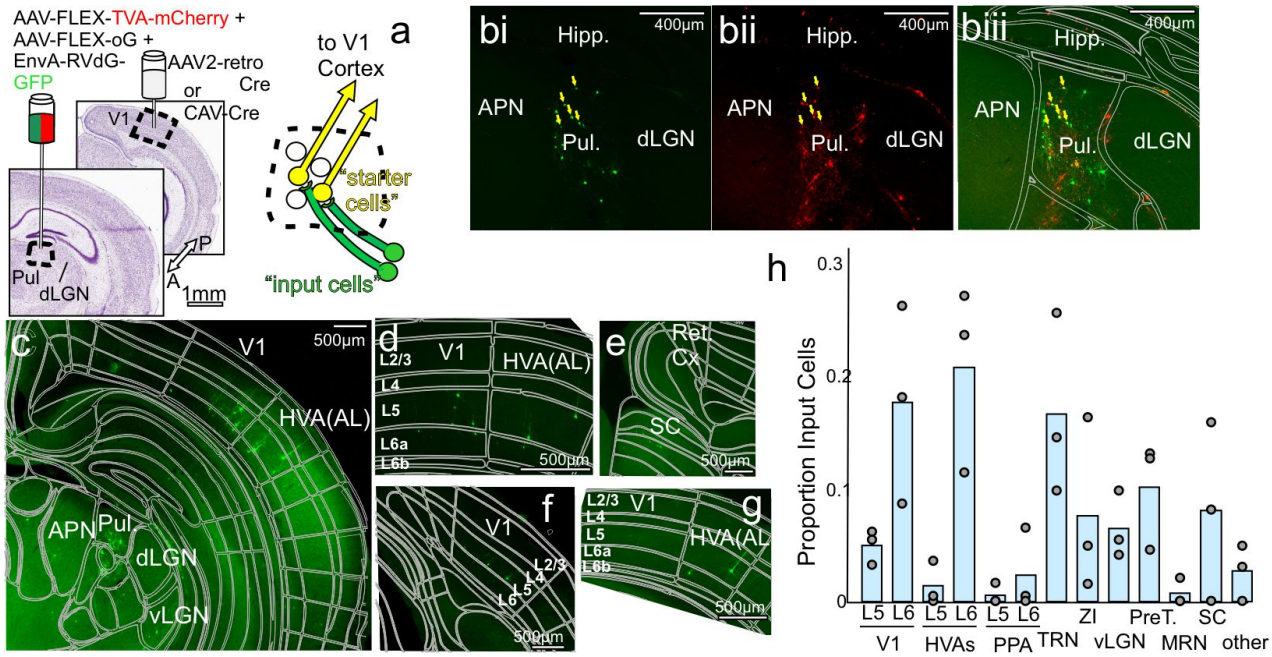

Figure 2.3: Retrograde transsynaptic tracing of inputs to the Pul → V1 pathway

(a) Schematic of the anatomical labeling strategy for labeling presynaptic inputs to the Pul → V1 pathway (see RESULTS and METHODS for details)
(b) Representative images of Pul, with GFP+ (Bi) and mCherry+ (Bii) cells double labeled (yellow arrows) in Pul only (overlay in Biii).
(c-g) Representative epifluorescence images of GFP+ presynaptic "input" cells, projecting to the Pul → V1 pathway. Cortical layers are labeled L2/3, L4, etc. Abbreviations: APN, Anterior pretectal nucleus, Ret. Cx, Retrosplenial cortex.
(h) Location of presynaptic GFP+ input cells as a proportion of the number of input cells found in each mouse (n = 3 animals).

Again, expected inputs were found in the inhibitory cells of thalamic reticular nucleus and zona incerta, as well as layer 6 of V1 and HVAs (Fig. 3c,d,g). Inputs from layer 5 of cortex were again observed in both V1 (Fig. 3c,d,f) and HVAs (Fig. 3c,d,g); SC also had cells innervating Pul → V1 (Fig. 3e). Notably, Pul includes at least 2 populations of Pul → V1 cells, one in the striate-recipient rostral pulvinar and one in the SC-recipient caudal and lateral Pul(Nakamura et al., 2015)·(Zhou et al., 2017). Slight variation in the anterior-posterior position of the rabies virus injections in Pul likely accounts for differences between animals in these results, with a slightly more anterior injection in one animal (Fig. S3b$_i$) resulting in more labeled inputs coming from

layer 5 of higher visual areas and a total lack of SC inputs, whereas a more posterior injection in another animal (Fig. S3b$_{ii}$) favored the labeling of SC inputs, and an intermediate position in a third animal (thus targeting both Pul → V1 populations) labeled both inputs from layer 5 of HVAs as well as SC inputs (Fig. 3h). Layer 5 of V1 provided input to Pul → V1 cells in all animals, in agreement with recent results that V1 can strongly drive some SC-recipient cells in the lateral Pul(Kirchgessner et al., 2021).

2.3.3: Layer 5 of multiple cortical areas can drive transthalamic feedback to S1 and V1

We used an optogenetics-assisted circuit mapping approach in layer 5 cre transgenic mice (Rpb4-cre) to validate the above anatomical findings and the expectation that layer 5 corticothalamic terminals should be strong drivers of thalamic activity (Sherman & Guillery, 2013)·(Kirchgessner et al., 2021)·(Reichova & Sherman, 2004). Specifically, a retrograde label (Fluororuby) was injected into all layers of S1 or V1, while an AAV expressing cre-dependent ChR2-eYFP was injected into candidate input cortical areas identified above. We then prepared acute slices in which we could target for whole cell recording the retrolabeled POm → S1 or Pul → V1 cells while optogenetically stimulating layer 5 axons from the candidate input area and thereby verify and describe the properties of these putative inputs.

Transthalamic pathways innervating S1. While making whole cell recordings from retrolabeled POm → S1 cells, focal laser stimulation of ChR2 axons or terminals from layer 5 of S1, S2, or M1 evoked depressing EPSCs (Fig. 4a-c), dependent on iGluRs with no evidence of a postsynaptic contribution of mGluRs (Fig. S1e), with a mixture of large and small amplitudes (Fig. S1c), all consistent with previous observations of layer 5 input to thalamus(Sherman, 2016)·(Sherman & Guillery, 2013)·(Mo & Sherman, 2019)·(Kirchgessner et al., 2021)·(Reichova

& Sherman, 2004). In the case of all layer 5 corticothalamic projections studied, optogenetic stimulation over either terminals or distant axons produced paired-pulse depression (Fig. S1a).

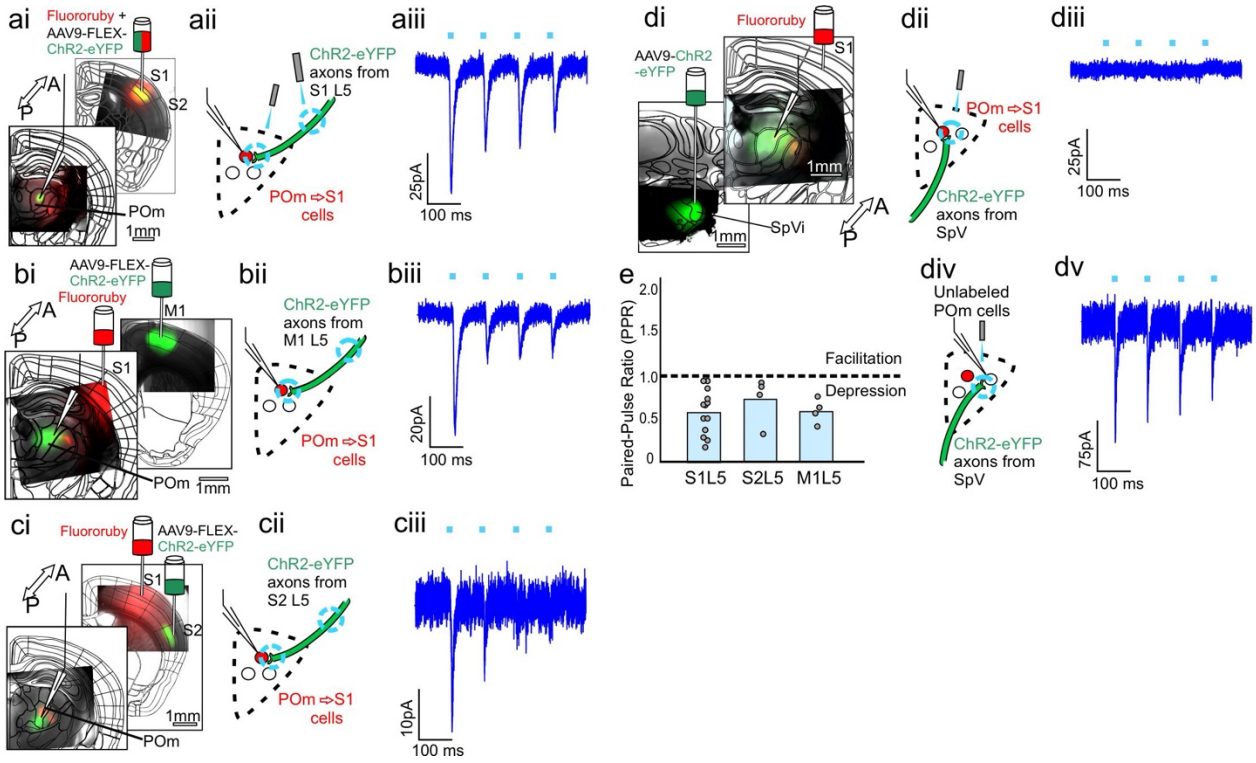

Figure 2.4: Layer 5 of S1, S2, or M1 can drive the POm → S1 pathway

(a) Ai: A schematic of the experimental strategy to validate layer 5 input from S1 to the POm → S1 pathway and epifluorescence images of injection and recording sites. A retrograde label (Fluororuby) was injected into S1 to label the POm → S1 cells (as well as other cells projecting to S1, e.g. in VPm) and an AAV expressing cre-dependent ChR2 (AAV9-pAAV-EF1a-DIO-hChR2(H134R)-EYFP-WPRE-HGHpA) was injected into the candidate input area, in this case S1 itself, in layer 5 cre (RBP4-cre) transgenic animals. The white recording pipette drawn over the epifluorescence image points to the recording site in POm, where red retrograde label and green layer 5 axons overlap. Aii: A schematic of the recording configuration. Labeled POm → S1 cells were targeted for whole cell recordings while photostimulating axons and/or terminals from layer 5 of S1. Aiii: Example voltage clamp recording of a POm → S1 cell during 10Hz photostimulation of axons from L5 of S1. All layer 5 responses were blocked with iGluR antagonists DNQX and APV (Fig. S1e).

(b) Bi and Bii: Same as in (a), but the cre-dependent ChR2 was expressed in layer 5 of M1. Biii: Example voltage clamp recording from POm → S1 cell during 10Hz photostimulation of axons from L5 of M1.

(c) Ci and Cii: Same as in (a and b), but the cre-dependent ChR2 was expressed in layer 5 of S2. Ciii: Example voltage clamp recording from POm → S1 cell during 10Hz photostimulation of axons from L5 of S2.

(d) di and dii: Same as in (a-c), except ChR2 was expressed in SpV (interpolaris region). diii: Example trace from a retrolabeled POm → S1 cell during photostimulation of axons from SpV. These failed to evoke EPSCs onto labeled POm → S1 cells (n=12 cells). Fiv and Fv: Example traces from an unlabeled POm cell of unknown projection identity during SpV photostimulation (n = 3).

(e) PPRs (2^{nd} EPSC amplitude / 1^{st} EPSC amplitude) for responses of retrolabeled POm → S1 cells to photostimulation of layer 5 of S1 (n = 13 cells), S2 (n = 4), or M1 (n = 4).

We had seen that SpV was not strongly labeled by transsynaptic retrograde tracing as a source of input to the POm → S1 sub-population (See Fig. 2). Consistent with that finding, while optogenetically activating SpV axons, we were not able to record EPSCs from retrolabeled POm → S1 cells, only from unlabeled cells in POm of uncertain projection identity (Fig. 2.4d).

These results fail to provide evidence for a feedforward pathway from SpV through POm to S1 but do confirm the existence of transthalamic feedback pathways whereby layer 5 of S1, S2, and M1 drive POm → S1 cells, which in turn modulate activity in S1.

Transthalamic pathways innervating V1. We used the same approach as in the somatosensory system to study the analogous circuits in the visual system. Thus, a retrograde label was injected into all layers of V1, while cre-dependent ChR2 was expressed in layer 5 of candidate input areas V1 and the HVA LM, the mouse cortical area most similar to V2 (see discussion) (Fig. 5). When targeting for whole-cell recording the retrolabeled Pul → V1 cells and optogenetically stimulating layer 5 axons from V1 or LM, we observed similar depressing EPSCs (Fig. 5a-c) dependent on iGluRs and no evidence of postsynaptic mGluRs, with a mixture of small and large amplitudes (Fig. S1d). These results confirm the existence of a transthalamic feedback pathway whereby layer 5 of V1 and LM drive Pul → V1 cells that in turn modulate activity in V1.

2.4: Discussion

Thalamocortical Drivers vs. Modulators

We found many similarities in the organization of HO thalamocortical circuitry in the somatosensory and visual systems. Firstly, HO thalamic terminals synapsing onto excitatory cells

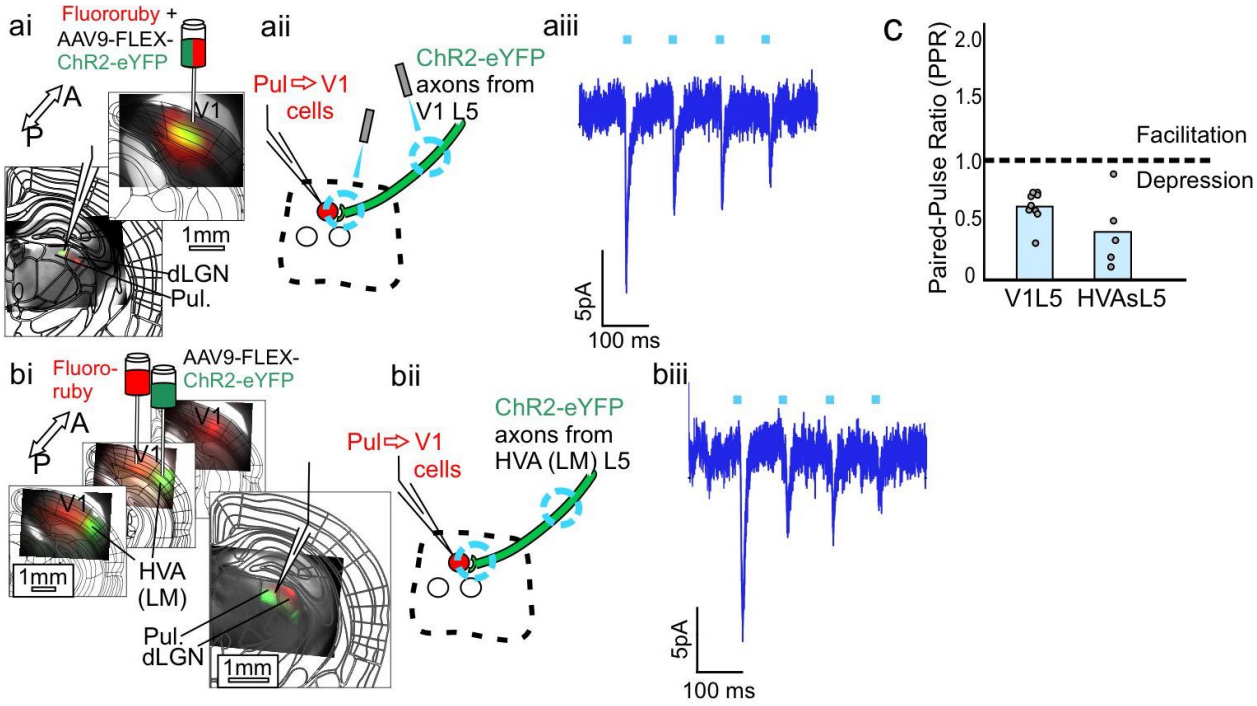

Figure 2.5: Layer 5 of V1 or HVA LM can drive the Pul → V1 pathway

(a) Ai: A schematic of the experimental strategy to validate layer 5 input from V1 to the Pul → V1 pathway and epifluorescence images of injection and recording sites. A retrograde label (Fluororuby) was injected into V1 to label the Pul → V1 cells (as well as other cells projecting to V1, e.g. in LGN) and an AAV expressing cre-dependent ChR2 (AAV9-pAAV-EF1a-DIO-hChR2(H134R)-EYFP-WPRE-HGHpA) was injected into the candidate input area, in this case V1 itself, in layer 5 cre (RBP4-cre) transgenic animals. The white recording pipette drawn over the epifluorescence image points to the recording site, where red retrograde label and green layer 5 axons overlap. Aii: A schematic of the recording configuration. Labeled Pul → V1 cells were targeted for whole cell recordings while photostimulating axons and/or terminals from layer 5 of V1. Aiii: Example voltage clamp recording of a Pul → V1 cell during 10Hz photostimulation of V1L5. All layer 5 responses were blockable with iGluR blockers DNQX and APV (Fig. S1e).

(b) Bi and Bii: Same as in (a), but the cre-dependent ChR2 was expressed in layer 5 of HVA LM. Biii: Example voltage clamp recording from a Pul → V1 cell during 10Hz HVAsL5 photostimulation.

(c) PPRs (2nd EPSC amplitude / 1st EPSC amplitude) for responses of retrolabeled Pul → V1 cells to photostimulation of layer 5 of V1 (n = 9 cells) or HVA LM (n = 5).

in S1 and V1 evoke small, facilitating EPSCs reflecting a low initial probability of neurotransmitter release (for review, see ref(Thomson, 2000)), and when stimulated at high frequency, evoke mGluR-dependent slow EPSPs, properties of glutamatergic modulator synapses(Sherman, 2016) ,(Sherman & Guillery, 2013),(Sherman & Guillery, 1998). This confirms and extends earlier work showing the same features for HO thalamic input to primary somatosensory and auditory

cortices(Viaene et al., 2011a)·(Viaene et al., 2011b). By comparison, HO thalamic terminals in higher cortical areas S2 and HVAs (with most such data deriving from LM) evoked stronger, depressing responses dependent on iGluRs only, consistent with descriptions of glutamatergic driver synapses(Sherman, 2016)·(Sherman & Guillery, 2013)·(Sherman & Guillery, 1998).

The observed pattern of physiological and pharmacological properties reported here has been a central part of the *Driver/Modulator* framework for classifying glutamatergic synapses. Within that framework, our data suggest HO thalamocortical projections modulate activity in S1 and V1, while driving activity in higher cortical areas. The underlying hypothesis for the functional significance of this is as follows: Driving projections provide temporally-precise excitation well suited to the efficient transfer of information and have been shown in many cases to do so (examples in(Kirchgessner et al., 2021)·(Diamond et al., 1992), reviewed in refs.(Sherman, 2016)·(Sherman & Guillery, 2013)). Glutamatergic modulatory inputs are so named because their effects resemble those of classical neuromodulators; these exert modulatory influence, likely affecting how postsynaptic targets process driver inputs(Sherman, 2016)·(Sherman & Guillery, 2013).

Along with PPRs, response amplitudes, and mGluR conductances, the size of synaptic terminals has also been used as an important criterion for the driver/modulator framework. Driver pathways form larger presynaptic terminals than do modulatory pathways(Mo & Sherman, 2019)·(Viaene et al., 2011a)·(Viaene et al., 2011b)·(Covic & Sherman, 2011)·(Petrof et al., 2015). Data presented here are consistent with these previous studies of thalamocortical terminal sizes. Pul terminals in V1 have generally been described as smaller than those in HVAs(Zhou et al., 2017), and POm terminals in S1 are smaller than those in S2(Viaene et al., 2011a).

Differences between FO and HO driving pathways

It is worth noting that the FO projection in the somatosensory and auditory systems (i.e., VPm → S1 and MGBv to A1) provide only driver input to the cells in layers 4-6, but for cells in layers 2/3, most receive modulator input, and the rest, driver(Viaene et al., 2011b). Consistent with this physiology, terminals from VPm in S1 were found to be smaller on average in layers 2/3 than in layers 4-6(Viaene et al., 2011b). For the purpose of comparing FO versus HO driving pathways, we acquired data from all layers 2-6 with emphasis on layers 2/3, and we found a very different pattern for the HO thalamocortical inputs to layers 2/3 of higher cortical areas. That is, HO thalamocortical input to all of the cells in layers 2/3 of S2 and HVAs were driver in nature (8 of 8 cells in layers 2/3 of S2 and 8 of 8 cells in layers 2/3 of HVAs, a significant difference from the driver / modulator ratio predicted by findings in the VPm → S1 and MGBv → A1 pathways in ref(Viaene et al., 2011b), $p = 3.95 \times 10^{-26}$, Chi square test with Yates correction). Consistent with that result, we recently showed that POm terminals in layer 4 of S2 (classical drivers) are not significantly larger than those in layers 2/3(Sampathkumar, Miller-Hansen, Murray Sherman, et al., 2021). This distinction between FO and HO driving projections is not without precedent, due to the recent finding that the inputs from POm to M1 in all layers, including layers 2/3, are exclusively driver(Mo & Sherman, 2019). Therefore, it may be a pattern common to other cortical circuitry that FO thalamic input strongly drives layer 4 and provides mixed inputs to layers 2/3 of primary cortical areas while HO thalamic input to higher cortical areas provides uniformly driving input to all layers.

Technical and experimental considerations

In our experiments using ChR2 to stimulate HO thalamic axons in cortex, we co-activated many individual thalamocortical afferents, and therefore postsynaptic responses may represent

combined responses, where responses to a minority of synapses of one type could be overwhelmed by those of the other type. That is, what we see as a driver (or modulator pathway) could contain small modulator (or driver) components. While possible in some cases, this type of error is unlikely to strongly affect our results for the following reasons. If a mostly driver pathway contained a significant representation of modulator inputs, we would expect to see measurable mGluR-dependent responses, which were never seen in our recordings from S2 or HVAs. A more likely scenario would be missing a sparse driver input among a mostly modulator pathway, since driver synapses are generally a smaller proportion of cortical synapses. However, the distribution of EPSC amplitudes across areas suggests that this did not happen to any appreciable extent in our recordings in S1 and V1, since these amplitudes were all quite small. Thus, while we cannot rule out some mixing of input types, if such contamination exists it is functionally meager.

Area LM was chosen as the extrastriate cortical area of mice to represent "higher visual areas," because it has been described as hierarchically next above V1(Wang et al., 2011)·(Siegle et al., 2021) and thus most closely resembles S2 hierarchically. It has also been identified specifically as a recipient of a feedforward transthalamic pathway (layer 5 of V1 → Pul → LM)(Blot et al., 2021). Most cortical recordings reported here in HVAs were made in LM, but Pul stimulation evoked similar responses in areas AL and AM (see Table S1).

Lastly, this project focused on thalamocortical synapses onto putative excitatory neurons, and it is important to note that projections from HO thalamus to primary sensory cortices also target inhibitory interneurons, particularly through their axon terminations to layer 1(Zhou et al., 2017)·(Fang et al., 2020), forming another, likely closely related mechanism for HO thalamic control of cortical activity. However, it was recently shown that the projection from POm to S2

targets only excitatory neurons(Sampathkumar, Miller-Hansen, Murray Sherman, et al., 2021), so this feature too may differ depending on hierarchical position or other circuit demands.

Sensory role of higher order thalamic projections to cortex

The current results complement work exploring HO thalamic contributions to sensory responses in somatosensory and visual cortex. Zhang et al.(Zhang & Bruno, 2019) recently showed that inactivating POm during whisker stimulation does not disrupt the initial sensory response in layers 2/3 of S1 (presumably dependent on driver projections from VPm) but abolishes persistent activity that typically lasts for hundreds of milliseconds, presumably dependent on the modulatory POm → S1 pathway, and possibly the mGluR conductances described here, which act over a similar timescale. Similarly in the visual system, deSouza et al.(de Souza et al., 2020) recently showed in the cat that silencing Pul altered sensory responses less in V1 than in a HVA, consistent with the proposed modulator/driver roles of pulvinar synapses in V1 vs HVAs.

Layer 5 cortical inputs to POm → S1 and Pul → V1

With regard to layer 5 cortical inputs to the POm → S1 and Pul → V1 pathways, transthalamic pathways between two separate cortical areas in the feedback direction had never been described before. We add to recent evidence showing the existence of reciprocal loops between a primary sensory cortical area and HO thalamus(Guo et al., 2020),(Juavinett et al., 2020),(Siegle et al., 2021), wherein HO thalamic cells projecting to one area receive input from layer 5 of that same area. Given that HO thalamic projections to S1 and V1 appear modulatory, these reciprocal loops do not violate Francis Crick's no-strong-loops hypothesis, stipulating that closed driver-driver loops are unlikely to exist in the brain since they would cause runaway

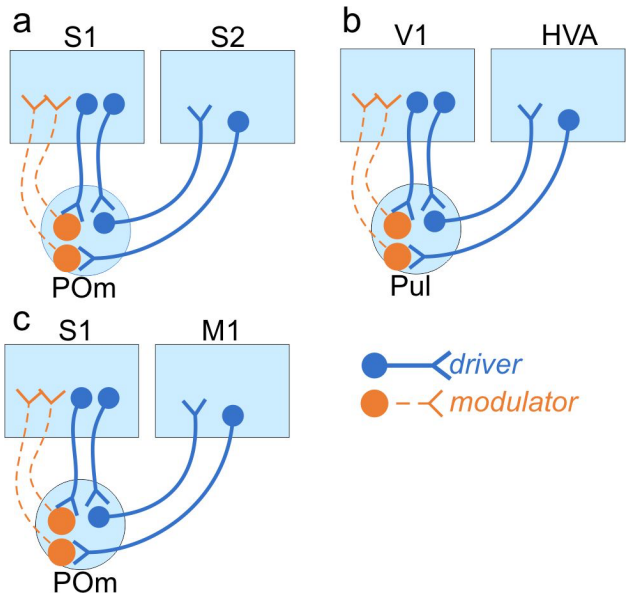

Figure 2.6: Summary of main conclusions.

In the feedforward direction, transthalamic pathways from S1 to S2 (a), V1 to HVAs (b), or S1 to M1 (c), all drive post-synaptic targets. Additionally, all inputs from layer 5 of cortex to HO thalamus are driver. However, the thalamocortical projections to primary cortical areas are modulatory, and are themselves driven by layer 5 of cortex in both reciprocal feedback pathways (layer 5 of S1 → POm → S1 and layer 5 of V1 → Pul → V1) as well as in transthalamic feedback from higher cortical areas to lower (layer 5 of S2 → POm → S1, layer 5 of M1 → POm → S1, and layer 5 of HVA LM → Pul → V1). Taken together, these data suggest that feedforward transthalamic pathways are mainly information-bearing, whereas feedback transthalamic pathways serve mainly a modulatory role.

excitation(Crick & Koch, 1998). It remains unclear if such reciprocal loops in thalamocortical processing are always modulatory in nature or if some indeed violate Crick's hypothesis.

As shown here and elsewhere(Guo et al., 2020), layer 5 terminals from S1 and V1 overlap convincingly with HO thalamic cells that send projections to S1 and V1 (Fig. 4a and 5a), while layer 5 terminals from higher cortical areas appear to overlap only partially with these cells (Fig. 4b,c and Fig 5b). However, our data show that these partially overlapping terminal fields from layer 5 of higher cortical areas also contribute driving input to some of the POm → S1 and Pul → V1 cells in adults, possibly via relatively few robust axons whose fluorescence signal is overwhelmed by nearby denser terminal fields. These synapses were not identified in a previous study of S1 and M1 connectivity through thalamus(Guo et al., 2020), likely due to small cortical injections allowing for topographical mismatch between S1 and M1. It is also the case that HO thalamic dendrites are not confined to well-defined input zones(Nakamura et al., 2015)·(Zhou et al., 2017). Therefore, while reciprocal loops undoubtedly contribute driving input to HO thalamus,

the current results suggest that these "closed" reciprocal loops exist nested within "open" transthalamic pathways connecting separate cortical areas in both the feedforward and feedback directions (see Figure 6).

Sub-cortical inputs to POm → S1 and Pul → V1

Several subcortical sources of input to HO thalamus were also identified in our g-deleted-rabies experiments (e.g., SC is known to send input to both POm and Pul) and we have attempted to understand where those subcortical inputs fit into our model of HO thalamus. In our optogenetics assisted circuit mapping experiment in the visual system, stimulating layer 5 cells from V1 or higher visual area LM evoked depressing EPSCs on retrolabeled Pul → V1 cells in both the striate-recipient (more rostral) Pul and SC-recipient (more caudal/lateral) Pul. These results are consistent with the idea that the rostral Pul → V1 population is cortically-driven without much sub-cortical input, much as in our findings on the POm → S1 pathway. On the other hand, the lateral Pul → V1 population can apparently still receive driving input from layer 5 of V1 and HVAs, but also receives dense subcortical innervation from SC. This view is also supported by the recent finding(Kirchgessner et al., 2021) that individual cells in lateral Pul can receive convergent driving input from layer 5 of V1 and SC.

In the somatosensory system, the sparsity of SpV input to the POm → S1 pathway was of particular interest to us. SpV densely innervates POm, and stimulation of SpV afferents evokes a mixture of driver and modulator-type responses in POm(Mo et al., 2017). However, our population-specific retrograde labeling failed to reveal a feedforward circuit from SpV to POm → S1 cells, and optogenetic SpV activation failed to evoke EPSCs onto retrolabeled POm → S1 cells. These data call into question the routing of the paralemniscal pathway through POm to S1, but agree with recent findings by El-Boustani et al.(El-Boustani et al., 2020) that suggest that SpV

input may preferentially innervate POm → S2 cells. It is not known whether the bottom-up inputs from SpV converge onto the same POm → S2 cells comprising the feedforward transthalamic pathway (S1 → POm → S2), or whether these are two separate populations of POm → S2 cells.

Transthalamic feedback pathways appear modulatory while feedforward ones appear to drive higher cortical areas

Our data suggest that feedback through thalamus is generally modulatory while feedforward transthalamic pathways can strongly drive activity in higher cortical areas. A few implications of this hypothesis are noteworthy.

First, the marked homogeneity of responses in each cortical area reported here (e.g. all driver-type responses from POm to S2 and Pul to HVAs) suggest the possibility that feedback through thalamus could skip over cortical areas of intermediate hierarchical position and only modulate primary sensory cortex. That is, no modulator-type responses were observed in areas S2 or LM, even though both are considered to be hierarchically secondary and therefore might be expected to receive feedback from even higher-order cortical areas. It may be true that areas highest along the cortical hierarchy indirectly exert feedback control over intermediate areas through transthalamic feedback modulation of primary cortex. Alternatively, cortical hierarchy in the mouse may be "shallower" than in other species, such that no cortical area is in a position to send robust feedback signals to S2 or HVA LM. Or lastly, feedback to these areas through HO thalamus may violate our hypothesis and act as a driver.

Secondly, while transthalamic communication from layer 5 of S1 → POm → M1 had been described previously to drive M1 activity(Mo & Sherman, 2019), our data verify the existence of a modulatory transthalamic pathway from layer 5 of M1 → POm → S1. Because POm projections

to M1 appear to be driver to all layers(Mo & Sherman, 2019) while POm projections to S1 are modulatory as described here, these two transthalamic pathways appear to have distinct functions. If the hypothesis is correct that feedforward routes through thalamus are drivers while feedback through thalamus is modulatory, this suggests a sensorimotor hierarchy in which S1 is lower than M1.

Lastly, these data also support the hypothesis that all direct corticocortical projections are paralleled by transthalamic pathways, now with our new evidence that this pattern also exists in the feedback direction. It has been suggested that in corticocortical communication feedforward projections are more specifically organized and robust while feedback projections are more diffuse and likely to be modulatory (reviewed in ref.(Callaway, 2004)). However, limited data have shown in the mouse that, in direct connections between V1 and HVAs as well as between A1 and A2, a mixture of driver and modulator inputs exist in both directions(De Pasquale & Sherman, 2011)·(Covic & Sherman, 2011), raising the possibility that purely feedforward driver and feedback modulator inputs are limited to transthalamic circuitry.

2.5: Materials and Methods:

Animals

Experiments were approved by the Institutional Animal Care and Use Committee at the University of Chicago. Transgenic mice expressing cre recombinase in layer 5 of cortex were bred by crossing male Rbp4-cre KL100Gsat/Mmcd mice (GENSAT RP24–285K21) with female C57BL6J mice. Cre positive offspring of both sexes were used in experiments, along with wild type C57BL6J mice (JAX).

Surgeries

Stereotactic injections of viruses and tracers were performed as previously described(Mo & Sherman, 2019) using a 0.5 uL Hamilton syringe. Surgeries for optogenetics were performed at p17-25 with coordinates in mm from bregma as follows (AP, ML, DV):

S1: -0.7,+3.1,-0.5; M1: +1.1,+1.2,-0.5; S2: -0.1,+4.0,-1.0; V1: -4.2,+2.2,-0.5; HVA-LM: -4.0,+3.5,-0.8; POm: -2.0,+1.25,-3.1; Pul: -1.8,+1.25,-2.4 SpV: -6.5,+1.9,-5.0.

Surgeries for G-Deleted rabies tracing were performed at age 8 weeks, with coordinates from bregma as follows:

S1: -0.8,+3.1,-0.5; V1: -4.2,+2.2,-0.5: POm: -2.2,+1.25,-3.2; Pul: -1.9,+1.25,-2.5

Viruses and Tracers

For optogenetics experiments, 50-90nl of AAV9-pACAGW-ChR2-Venus (Addgene, 20071-AAV9) was injected to allow photostimulation and visualization of thalamocortical projections, 200nl were injected for SpV, and 120-300nl of AAV9-pAAV-EF1a-DIO-hChR2(H134R)-EYFP-WPRE-HGHpA (Addgene, 20298-AAV9) was used to allow photostimulation and visualization of layer 5 corticothalamic projections in a cre-dependent fashion, depending on the injection target. Three weeks were given for expression before recordings were obtained.

For retrograde labeling of thalamocortical projections to cortex, 150-300nl of 10% Fluororuby (Thermo Fisher: D1817) in PBS was injected into appropriate cortical regions. Fluororuby is known to label cell bodies and sometimes processes without altering electrophysiological properties(Mo & Sherman, 2019).

For G-deleted rabies tracing experiments, a protocol was developed using minimal viral volumes for sparse labeling, as described below. 200nl nl of either CAV2-CMV-Cre (Montpellier Vectorology, Institut de Génétique Moléculaire de Montpellier) or AAVretro-Ef1a-Cre (Salk Inst., 55636) was injected in cortical areas S1 or V1 to deliver cre retrogradely to higher order thalamus. At the same time, 80nl of a 1:1 mixture of AAV8-CAG-FLEX-TCB (TVA-mCherry) and AAV8-CAG-FLEX-oG-WPRE-SV40-PA (Optimized G) (Salk Inst., 48332 and 74292, respectively) was injected into the relevant HO thalamic nucleus, POm or Pul. After 3 weeks allowing for expression, 80nl EnvA-G-Deleted Rabies-eGFP (Salk Inst., 32635) was injected also in POm or Pul.

Strategy for G-Deleted-RV Tracing

For this output-defined G-deleted-rabies tracing strategy(Schwarz et al., 2015)·(Callaway & Luo, 2015), there is always a concern that a small percentage of cells in the "starter" region (here POm and Pul) may express TVA-mcherry and G in a cre-independent fashion without receiving cre from the relevant projection region, and thus retrogradely labeling spurious "input" cells merely projecting to the region. Likewise, there is a possibility for a small percentage of cre-expressing cells in the projection regions, S1 and V1, to pick up the cre-dependent TVA-mCherry and pseudotyped RV-GFP in thalamus, allowing for spurious GFP+ labeling in cortex. To avoid this second scenario, all cortical GFP+ input cells were screened for Mcherry labeling (they should be GFP+ Mcherry- unless incidental retrograde labeling from thalamus occurred). No Mcherry labeling was observed outside of thalamus in the animals included in analysis. To minimize the probability of either pitfall affecting results, a protocol was designed to sparsely label the relevant "starters" and "inputs" with relatively small viral volumes. This approach allowed careful manual screening of each labeled cell through a 10x objective, and any data was discarded from animals

with any spuriously double-labeled cells in cortex or starter cells in the neighboring FO thalamic nuclei outside of the target zone.

Images taken through a 5x objective were overlaid with the Allen Institute Mouse Brain Atlas (.brain-map.org/experiment/thumbnails/100048576?image_type=atlas) for assessment of subcortical and cortical areas. Cortical layers were determined similarly and using distance from the pia (dorsal surface of cortex). Negative controls without Cre were also assessed and found to have small amounts of mCherry labeling in thalamus, but no cre-independent GFP labeling of inputs (Fig. S2 and 3).

While this approach limits the quantitative assessment of large numbers of labeled cells, such assessments can be affected by poorly understood cell-type biases. We find this sparse labeling approach yields more reliable qualitative data about synaptic inputs to heterogeneously organized brain areas such as HO thalamus.

Anatomical Tissue Preparation and Microscopy

As described previously(Mo & Sherman, 2019), animals were transcardially perfused with phosphate-buffered saline followed by 4% paraformaldehyde in phosphate-buffered saline, pH 7.4. The brain was extracted and postfixed in 4% paraformaldehyde for at least 12 hours before transferring to a cold 30% sucrose solution for >48 h. Brains were then cryosectioned coronally at 40 μm thick on a sliding microtome.

Brain sections were mounted on Superfrost Plus (Fisher Scientific) slides and coverslipped with DPX or Vectashield with DAPI (Vector Laboratories). A microscope with a 100 W mercury lamp with fluorescence optics (Leica Microsystems) was used to image the sections and photos were taken with a Retiga 2000 monochrome CCD camera and Q Capture Pro software (Qimaging).

Leica TX2 filter cubes (excitation 560 nm, emission 645 nm, dichroic 595 nm) were used to visualize Fluoro-Ruby and mCherry fluorescence, L5 filter cubes (excitation 480 nm, emission 527 nm, dichroic 505 nm) were used to visualize GFP and eYPF fluorescence. Q Capture Pro software and FIJI (NIH) were used to overlay images and adjust brightness and contrast. High-resolution photomicrographs of input cells were captured with LAS AF Leica software on a Leica SP5 Tandem Scanner Spectral 2-phtoon confocal microscope.

Electrophysiological Slice Preparation

Animals were anesthetized to be nonresponsive to toe pinch and transcardially perfused with 4 ml of cold oxygenated (95% O_2, 5%CO_2) artificial cerebrospinal fluid , which contained the following (in mM): 125 NaCl, 25 $NaHCO_3$, 3 KCl, 1.25 NaH_2PO_4, 1 $MgCl_2$, 2 $CaCl_2$, and 25 glucose. The brain was extracted, blocked in accordance with the desired slice angle (see below), glue-mounted on a vibratome platform (Leica), and sliced in cold (1–4°C), oxygenated slicing solution containing the following (in mm): 2.5 KCl, 1.25 NaH_2PO_4, 10 $MgSO_4$, 0.5 $CaCl_2$, 25 $NaHCO_3$, 11 glucose, and 206 sucrose. Slices were cut at 420 um thickness.

While many recordings could be made in coronal slices, to facilitate the distant optical stimulation of presynaptic axons, for recordings in cortex, many brains were cut at angles preserving some but not all of the complete circuit, referred to as “pseudo-connected” slices. For somatosensory thalamocortical projections, brains were cut at 55° from the midline and 10° from the horizontal to preserve thalamocortical projections(Agmon & Connors, 1991). For visual thalamocortical projections, brains were cut at 55° from horizontal as in ref.(MacLean et al., 2006). In experiments recording in thalamus, slices were made coronally.

Brain slices were then transferred to 33°C oxygenated artificial cerebrospinal fluid that was allowed to return to room temperature thereafter. Recovery in artificial cerebrospinal fluid

occurred in the dark for at least 1 hour and all slicing and patching were performed in minimal light.

Whole Cell Recordings

Slices containing the relevant regions of thalamus or cortex were visualized using differential interference contrast with a Axioskop 2FS microscope (Carl Zeiss). Fluorescent ChR2 expression was confirmed using the 5× air objective with a fluorescein isothiocyanate filter (set 37; Zeiss) and Fluororuby-labeled cells were identified under 40× magnification with a rhodamine filter (set 15; Zeiss). Recordings were made with a Multiclamp 700B amplifier and pCLAMP software (Molecular Devices). Recording glass pipettes with 4–6 MΩ resistance were filled with intracellular solution containing the following (in mm): 117 K-gluconate, 13 KCl, 1 $MgCl_2$, 0.07 $CaCl_2$, 10 HEPES, 0.1 EGTA, 2 Na_2-ATP, 0.4 Na-GTP, pH 7.3, 290 mOsm, and 0.5–1 dinitrostilbene-2,2-disulfonic acid (a $GABA_A$ antagonist). Pharmacological inactivation of iGluRs was induced by bath application of 50 μM DNQX and 100 μM AP5, while group I mGluRs were blocked with 40 μM LY367385 and 30 μM MPEP. The locations of each patched cell within cortex was imaged along with its recording pipette and assigned to a layer by distance from pia and white matter, along with differences in transmitted brightness under DIC, and relation to other relevant landmarks (e.g., barrels in S1). Transition areas near laminar borders were avoided. Once whole cell recordings were achieved, the excitatory identity of thalamic relay cells were verified by characteristic responses to current injections (rebound bursts in response to hyperpolarization). The excitatory identity of cells in cortex was verified by layer and area-specific responses to positive and negative current injections which easily distinguish GABAergic interneurons(Scala et al., 2019), as well as by size and shape (all excitatory cells were pyramidal with the exception

of S1 layer 4), as described previously(Viaene et al., 2011a)·(Viaene et al., 2011b)·(Scala et al., 2019).

Optogenetic stimulation was delivered using a 355nm laser (DPSS: 3505-100), controlled with galvanometer mirrors (Cambridge Technology) focused on the slice through a 5× air objective using custom software in MATLAB (MathWorks). 4 pulses of 1ms duration were delivered at 100ms ISI during recordings in voltage clamp. Laser intensity at the slice was varied by a neutral density filter wheel before in the beam path. Stimulations were attempted at low intensity before slowly increasing until postsynaptic responses were observed. At a typically used intensity for near-threshold activation, the beam produced an 80 μm diameter illuminated spot with a power of 5mW at the level of the slice using an optical power meter (Thorlabs). Focal laser stimulation was directed either over the patched cell to activate the ChR2-expressing presynaptic terminals or at a distance of >300 μm away to activate distant ChR2-expressing axons in accordance with previous work[18]. For high-frequency optogenetic stimulation, 20 pulses of 1ms duration were delivered at 12 ms ISI (83Hz), and responses were recorded in current clamp. Electrical stimulation of POm → S1 pathway was achieved with a 2 × 1 matrix tungsten bipolar electrode with 115 μm separation (FHC) placed along labeled thalamocortical fibers in the internal capsule. Four 0.1-ms-long pulses were delivered at 10 Hz.

Data Analysis and Statistics

Electrophysiological data were collected using custom MATLAB software and analyzed using RStudio (v1.3.959). The amplitude of responses to stimulation pulses was measured by subtracting the average value for 20ms before the delivery of a pulse (baseline) from the maximum value of the peak. The PPR was calculated by dividing the amplitude of the second pulse by that of the first pulse. Statistical analyses were also conducted in RStudio. All comparisons between

groups are Mann-Whitney U tests, except for the comparison of the driver / modulator ratio observed in our recordings in S2 and HVAs with the driver / modulator ratio from FO thalamic stimulations recorded in S1 and A1 from ref(Viaene et al., 2011b), which used a Chi square test with Yates correction. Image analysis was conducted in FIJI (NIH), and figures were produced using Corel Draw (v21).

2.6: Acknowledgments

This research is supported by grants from the National Institute of Neurological Disorders and Stroke: NS094184 and NS113922. Also, A.M.-H. is supported by a fellowship from the National Eye Institute: EY028812. We thank John Maunsell for his helpful comments in the preparation of this manuscript.

2.7: Appendix A: Supplemental Figures

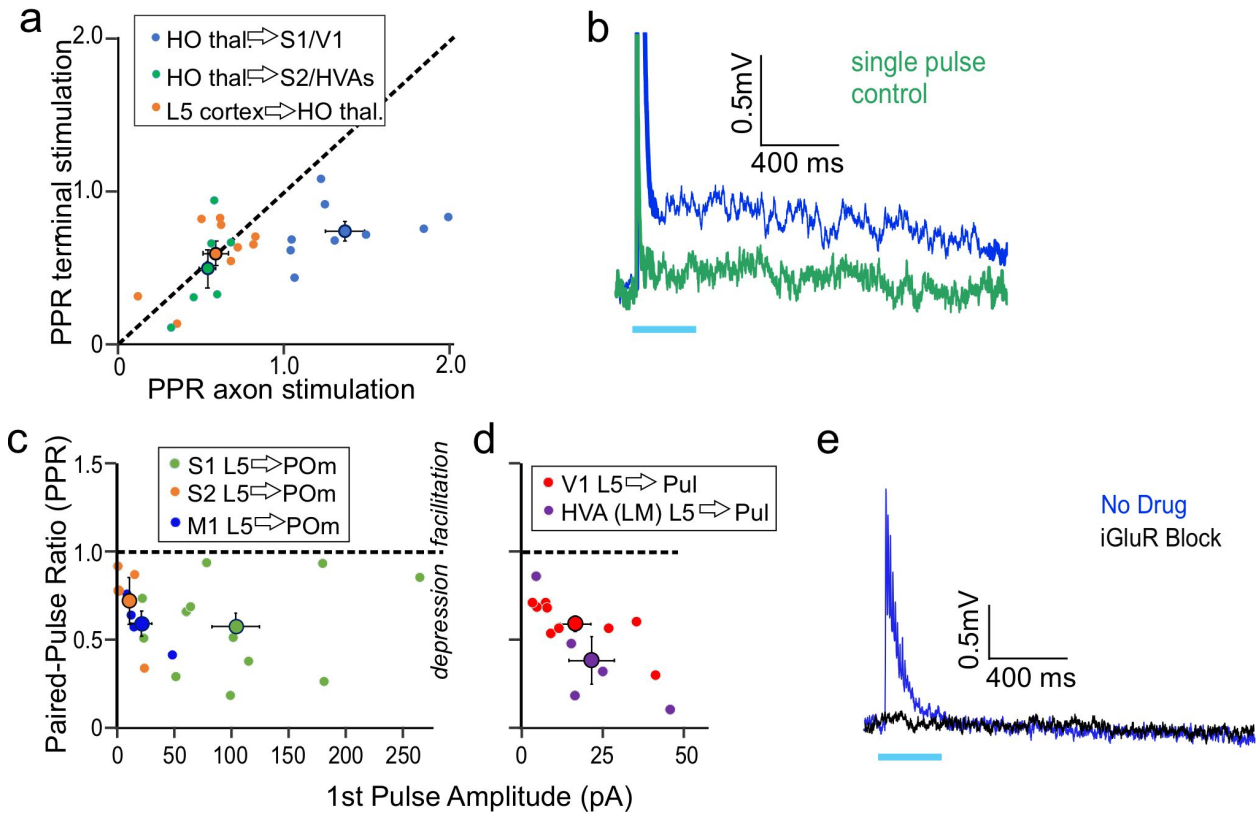

Supplemental Figure 1: Electrophysiology supplement

(a) PPRs when data when axon stimulation and terminal stimulation were collected from the same cell. Larger dots represent the mean for each group with bars for SEM. On average, depressing responses (PPR<1) were not changed and fall along the unity line. However, facilitating (PPR>1) responses to axonal stimulation were changed to depression on average (blue dots represent data from recordings in S1 and V1).

(b) A representative example of an mGluR response to high-frequency stimulation in V1 cortex (blue trace). When the repetitive stimulation is replaced with a single pulse at the same intensity (green trace), the initial fast depolarization remains unaffected while the slow mGluR-dependent phase is abolished, consistent with the finding that repetitive stimulation is required for mGluR recruitment[30].

(c) The PPR and 1st EPSC amplitudes of POm → S1 cells' response to a series of 10Hz optogenetic stimulations of layer 5 of S1 (n=13), S2 (n=4), or M1 (n=4). Large dots represent the means of each group and error bars represent SEM.

(d) The PPR and 1st EPSC amplitude of Pul → V1 cells' response in a series of stimulations of layer 5 of V1 (n = 9) or HVA LM (n = 5). Large dots represent the means of each group and error bars represent SEM.

(e) A representative example of a HO thalamic cell's response to high frequency stimulation of a layer 5 axon or terminal. Depolarization is abolished with iGluR blockers alone.

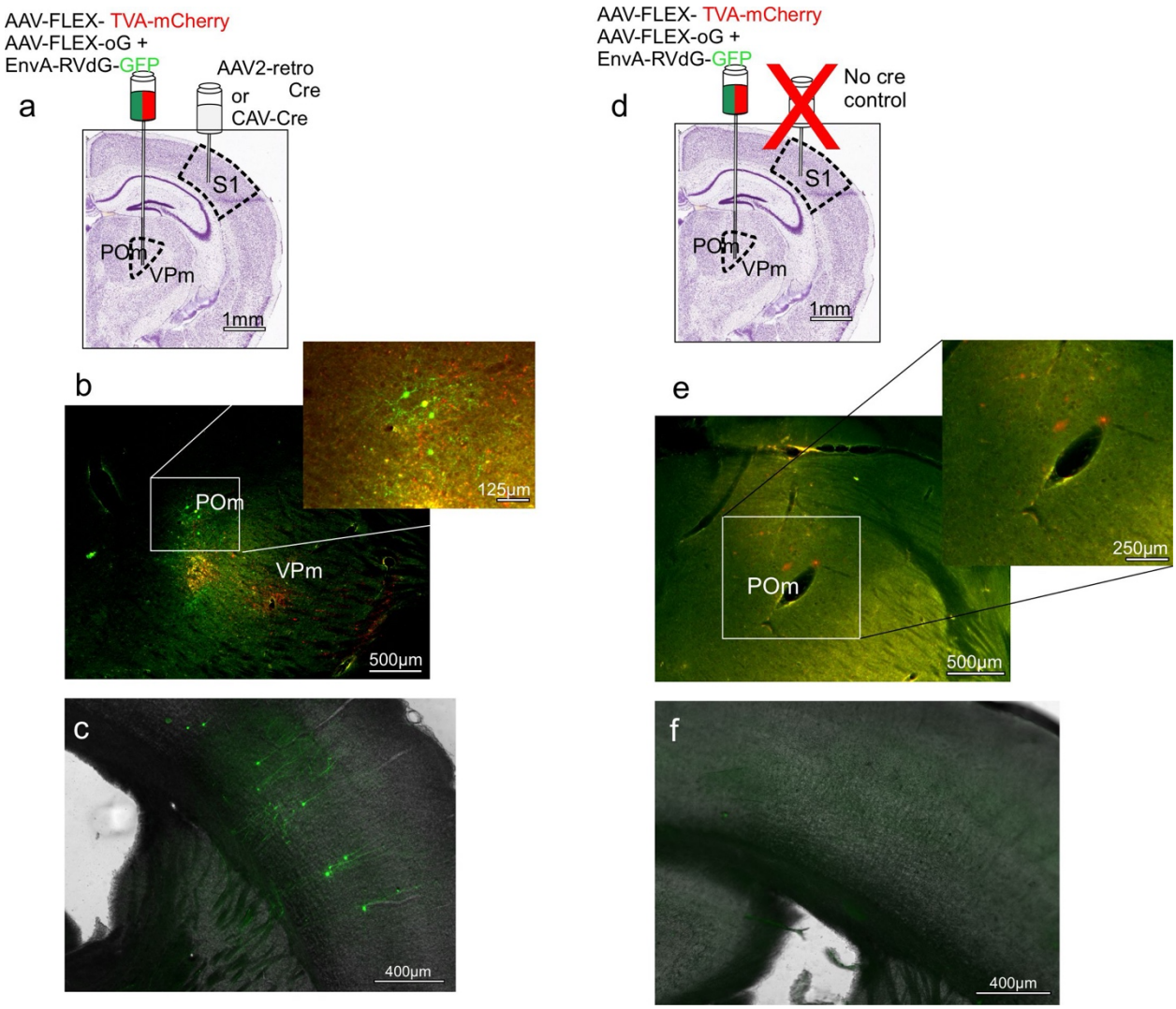

Supplemental Figure 2: G-deleted rabies labeling of pre-synaptic inputs to POm → S1 is dependent on cre recombinase

(a) Experimental strategy for G-deleted rabies tracing of inputs to the POm → S1 pathway, with retrograde cre injection in S1, as in Fig. 2.
(b) Example starter cells in POm
(c) Example retrogradely labeled input cells in somatosensory cortex.
(d) Same as in (a), except without the virus delivering cre recombinase.
(e) Sparse labeling may be present in POm, but no double-labeled starter cells
(f) Pre-synaptic inputs to POm are not labeled.

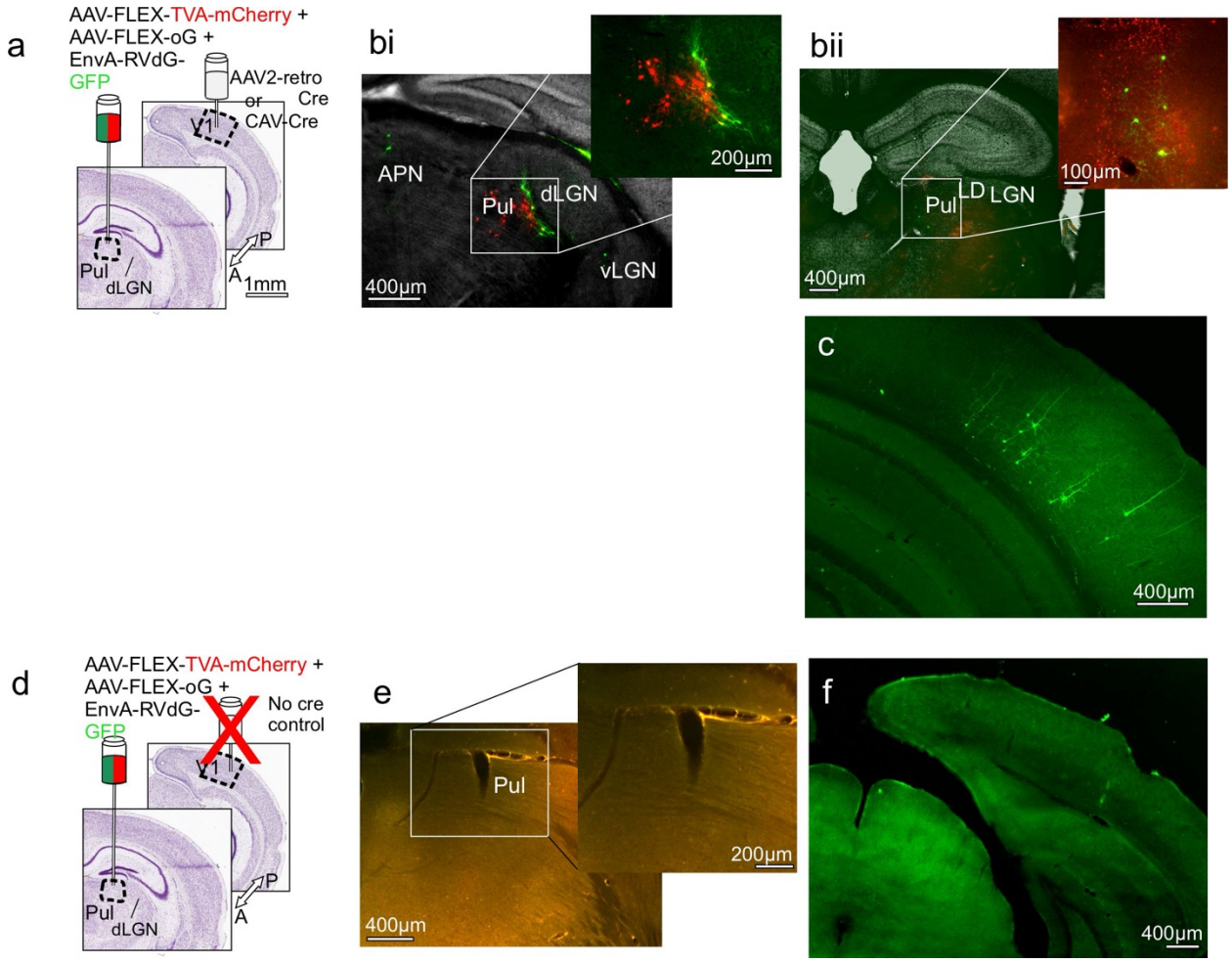

Supplemental Figure 3: G-deleted rabies labeling of pre-synaptic inputs to Pul → V1 is dependent on cre recombinase

(a) Experimental strategy for G-deleted rabies tracing of inputs to the Pul → V1 pathway, with retrograde cre injection in V1, as in Fig. 3.
(b) Example starter cells in more caudal (bi) and rostral (bii) Pul of separate animals
(c) Example retrogradely labeled input cells in visual cortex.
(d) Same as in (a), except without the virus delivering cre recombinase.
(e) Sparse labeling may be present in Pul, but no double-labeled starter cells
(f) Pre-synaptic inputs to Pul are not labeled.

2.8: Appendix B: Supplemental Table

Table S1: Thalamocortical response properties by cortical area and layer

Cortical Area	Layer	n	Mean 1st Pulse Ampl.	Mean PPR
S1 pooled	all	12	12.00	1.27
S1	2/3	6	12.19	1.36
	4	1	19.14	1.29
	5	4	11.64	1.09
	6	1	5.13	1.38
S2 pooled	all	13	37.81	0.64
S2	2/3	8	44.45	0.63
	4	2	36.27	0.58
	5	2	26.82	0.62
	6	1	9.67	0.89
V1 pooled	all	12	13.27	1.30
V1	2/3	5	12.01	1.26
	4	1	8.81	1.13
	5	4	17.50	1.51
	6	2	10.18	1.10
HVAs pooled	all	16	38.76	0.57
HVA (LM)	2/3	4	61.29	0.67
	4	3	29.68	0.37
	5	2	10.82	0.77
	6	1	8.52	0.70
HVA (AM)	2/3	2	74.18	0.54
	4	1	19.40	0.49
	6	1	42.85	0.45
HVA (AL)	2/3	2	22.58	0.55

CHAPTER 3: GENERAL DISCUSSION

3.1 Functional Implications of Glutamatergic Modulators

We have shown that HO thalamic inputs to primary sensory cortex show several properties of synapse physiology and pharmacology associated with glutamatergic modulator pathways and argued that these pathways would therefore be well-suited to modulating excitatory activity in S1 and V1. Aside from the association in the literature between these parameters and synaptic efficacy (PPR, response amplitudes, and mGluR responses as reported here, as well as pre-synaptic terminal sizes as referenced above), it is worth noting in more detail lines of evidence supporting the suggestion that such pathways can functionally exert modulatory influence over sensory-evoked activity in intact brains.

In the visual system, silencing of HO nucleus Pul directly deprives a given cortical area of its Pul inputs, but also indirectly deprives it of corticocortical inputs dependent on Pul activity. Therefore, experiments silencing the Pul as a whole can be interpreted only with this major caveat. In a recent study using anaesthetized cats (de Souza et al., 2020), silencing of Pul led to changes in the neural responses to drifting gratings in cortical areas 17 and 21a (homologues of primate V1 and V4 respectively)(Payne, 1993). In both areas, pharmacological inactivation of Pul caused extracellularly recorded responses of single cells to be either suppressed or facilitated with a slight bias for facilitation in superficial layers of area 17 and suppression in deep layers. However, this study also assessed responses to a number of different contrasts and used these to assess a "contrast response function" for each area. The largest changes were in responses to higher contrasts, and notably the contrast response function was only shifted very slightly in area 17 but much more strongly in area 21a. One simple interpretation of this result is that Pul exerts stronger control over cortical activity in a HVA than it does over V1. However, the mixture of suppression and

facilitation of responses highlights the complex push-pull nature of thalamocortical interactions. It has been shown that FO and HO thalamus can innervate excitatory cells and inhibitory interneurons of cortex (more on this below). Therefore, it is not likely that Pul contributes to sensory responses in cortex by simply adding excitation to the relevant cortical column, but rather affects the activity of a distributed cortical network in more nuanced ways.

Another relevant study was done in anaesthetized galagos (a prosimian primate) (Purushothaman et al., 2012), and showed very different results. Similarly, visual responses to drifting gratings were assessed in V1 before and after pharmacological inactivation of Pul. Curiously, in galagos, inactivation of Pul was associated with a universal suppression of superficial V1 responses to all orientations. The degree of suppression of individual cell's responses was highly variable with most responses being suppressed very slightly and some being almost completely silenced. While both this study (Purushothaman et al., 2012) and the previously mentioned (de Souza et al., 2020) are generally consistent with the idea that Pul exerts modulatory influence over V1, the strikingly different results of Pul inactivation in cats and galagos are difficult to reconcile. It may be that these species show differential recruitment of inhibitory interneurons in V1, with Pul only contacting excitatory cells in galagos, but this is not the case in other primates (Rockland, 2019) or rodents (Fang et al., 2020). Experimental differences may be relevant, for example the forms of anesthesia used (intraperitoneal urethane in galagos and inhaled isoflurane in cats) may affect sensory responses in these animals differently. Anesthesia is known to affect sensory responses in cortex (Shumkova et al., 2021), and strongly affect the activity of HO thalamus (Masri et al., 2008), which is why it is much preferred in modern studies that animals be awake or lightly sedated (Constantinople & Bruno, 2011). In either case, we can conclude that

sensory-evoked responses in V1 are clearly affected by the silencing of Pul, although there has been some disagreement about the direction of that change, whether net suppression or facilitation.

Recent studies in rodents have had more success in specifically measuring and manipulating the Pul projection to V1 without altering other Pul projections. A study of calcium activity in the Pul axons in V1 of awake mice showed that their activity was closely associated with visuo-motor discrepancies (experimentally mismatching movement and visual feedback) (Roth et al., 2016), supporting the idea that HO thalamus encodes mostly movement-related sensory information. Also recent bi-directional optogenetic manipulation of Pul → V1 axons in mice during visual stimulation showed that activation of Pul slightly decreased responses in V1 layers 2/3, while inhibition led to a slight facilitation of responses (Fang et al., 2020). This paper also implicated Pul generally in enhancing feature selectivity and contextual modulation of responses in V1. These modulatory effects could be mediated by Pul synapses onto inhibitory interneurons in V1 as suggested in (Fang et al., 2020), but they are likely also dependent on the glutamatergic modulator Pul synapses onto excitatory cells described in Chapter 2. Such synapses would have dynamic effects on post-synaptic activity over a wide range of activation frequencies (dependent on paired-pulse facilitation and group I MgluRs), and could exert influence over longer time windows matching the longer time-course of contextual modulation in V1 (Zipser et al., 1996)(Alexander & Wright, 2006).

HO thalamocortical interactions of the somatosensory system are less-well studied in primates and carnivores, but studies have been conducted to assess the contribution of POm to S1 responses in rodents. As mentioned earlier, a recent study (Zhang & Bruno, 2019) silenced mouse POm and showed that S1 responses to whisker stimulation retained their short-latency initial depolarizations but lost a longer-lasting (hundreds of milliseconds) persistent phase of activity that

was dependent on POm. This result is also consistent with the view that HO thalamic input in this case is modulatory, since inputs described as glutamatergic modulators are thought to alter the way other driver inputs are processed over a longer time window. As in the visual system, we showed the presence of group I mGluRs at POm → S1 synapses, which are known to activate post-synaptic targets over hundreds of milliseconds, and therefore may be the mechanism mediating this prolonged increase of excitability. POm, similarly to Pul, is also known to contact inhibitory interneurons in S1 (Audette et al., 2019), suggesting a similar push-pull relationship with the cortical network.

3.2 Patterns of HO Thalamic Inputs / Outputs

This project also explored the synaptic inputs to the Pul → V1 and POm → S1 pathways in an attempt to understand which are the relevant driving inputs. In the visual system, our projection-specific retrograde tracing experiment labeled many of the same inputs as traditional retrograde labeling, a similar result as shown recently in tracing inputs to the Pul → HVA (LM) pathway (Blot et al., 2021). Our experiment in the somatosensory system labeling inputs to the POm → S1 pathway similarly labeled most inputs to POm, with the notable exception of SpV, which agrees with a recent anatomical result from anterograde tracing of SpV inputs (El-Boustani et al., 2020). With this one exception (SpV axons avoiding POm → S1 cells), it may be tempting to conclude that the sub-populations of HO thalamic cells projecting to different cortical areas are not separate populations, but merely branched axons from the same set of HO thalamic cells receiving a homogeneous set of inputs. There is in fact disagreement about the degree to which HO thalamocortical projections represent separate populations. There is a loose anatomical organization within HO thalamic nuclei of projection patterns, but there appear to be many

exceptions. Retrograde labeling experiments where different retrograde labels are put in different cortical areas and then double-labeled cells in HO thalamus are counted have been conducted, and the numbers of double labeled cells are always quite low (e.g. 4-6% in the Pul of mice (Juavinett et al., 2020) or 5-12 % in the macaque (Kennedy & Bullier, 1985)). These results are generally biased, however, by the low efficiency of retrograde labels. Another approach has been anatomical reconstructions of entire projection neurons including their branches, however this work is difficult and rarely undertaken. The few such studies that exist do indeed show examples of both POm (Ohno et al., 2012)(Rodriguez-Moreno et al., 2020) and Pul neurons innervating multiple cortical areas (Rockland et al., 1999)(Rockland, 2019). In some cases, (Rodriguez-Moreno et al., 2020) have even shown branches from one POm axon innervating both M1 and S1 and showing functionally divergent synapse properties (those of a driver in M1 and those of a modulator in S1), an example of a, "multi-specific" thalamocortical projection. This pattern suggests that the functional properties of a thalmocortical synapse are dictated by the terminal area and not necessarily by the identity of the pre-synaptic cell. It follows that aside from the division of inputs (as in the SpV axons avoiding POm → S1 cells), in such a system the different projections need not arise from separate cell populations. Therefore, while HO nuclei do contain loose anatomical sub-divisions with projection preferences, it is still not quite clear how commonly HO thalamic projections to cortex branch to innervate multiple areas, and single cell reconstructions show us irrefutably that some of them do so.

It may not be so surprising then that we have found in this project that HO thalamic cells projecting to primary cortical areas can receive driving input from layer 5 of many cortical areas (primary and higher). While it appears that projection populations in HO thalamus do sometimes receive different patterns of inputs, given that there are many cells projecting to multiple cortical

areas, the discrete organization of inputs into separate output channels cannot be complete. It is likely the case that some HO thalamic cells receive only one type of driving input (particularly in the somatosensory system, where the S1 layer 5 terminals are located in an anatomical field matching almost perfectly the location of the POm → S1 cells, see Fig 2.4a1), however they need not receive entirely discrete patterns of inputs, since these cells occasionally project to other cortical regions as well via branched axons.

It is also possible for a single HO thalamic cell to receive converging driving inputs from multiple regions, as shown recently using cre-dependent electron microscopy (Sampathkumar, Miller-Hansen, Sherman, et al., 2021). In some cases, it should be noted, the "no-strong-loops" hypothesis would predict an omission of an input, based on our data. For example, a POm cell projecting to S1 alone may receive convergent driving input from S1 layer 5 and S2 layer 5. Since we have shown that POm modulates all layers of S1, such a cell would form both a reciprocal modulatory loop with S1 and provide transthalamic feedback modulation from S2 to S1. However, we have shown that the POm projection to S2 drives post-synaptic targets in all layers. Therefore, if a POm → S2 cell were to receive a layer 5 driving input from S2, that would form a driver-driver loop, in violation of the, "no-strong-loops" hypothesis. Further anatomical studies will reveal whether or not such pathways exist.

3.3 Remaining questions

Given their organizational conservation across systems, it is likely that reciprocal and non-reciprocal connections between cortex and HO thalamus are critical to the stability of cortical representations and are integral to the flow of information in the brain. While these data have given us a slightly clearer picture of some details of HO thalamocortical interactions, many questions

remain. Here we speculate about answers to these in the hopes that future study will provide concrete evidence: *Why do cortical areas that are directly connected to each other have additional transthalamic connections through HO thalamus in both feedforward and feedback directions?* In contrast to direct cortico-cortical communication, activity passed through HO thalamus passes through some extra steps that may perform important processing functions on that activity. For one, thalamic activity is strongly controlled by the inhibitory networks of zona incerta (for HO thalamus) and the thalamic reticular nucleus (both FO and HO thalamus). These inhibitory networks would be able to gate the flow of transthalamic activity based on arousal or other behaviorally-relevant brain states, while cortico-cortical information transfer would not be so gated. We have also mentioned to convergence of driver inputs from different cortical regions onto individual cells of HO thalamus. In (Sampathkumar, Miller-Hansen, Sherman, et al., 2021), we showed that over half of POm cells reconstructed received input from layer 5 of S1 and M1 cortex, suggesting that this type of convergence may in fact be quite common. Therefore, it may also be the case that transthalamic pathways allow information to be integrated with driving inputs from other sources before sending a "multiplexed" signal back up to cortex.

Does this parallel pattern always exist, or are some cortical areas connected by just direct or transthalamic pathways? In all cases where two cortical areas are connected directly and a transthalamic pathway has been looked for, one has been found, now even in the feedback direction. A more complete anatomical picture of connectivity through HO thalamus will be necessary before we can know whether this is always the case or not. It would be very interesting to understand the differences between connections that do not require a parallel route through thalamus and those that do, and it would perhaps give us an important clue regarding their function.

However, it may be that a transthalamic pathway parallels all direct cortico-cortical connections, and that it is necessary architecture supporting communication between cortical areas.

How do transthalamic and cortico-cortical routes of information re-combine in target areas? It would also give us clues about the function of transthalamic pathways if we could understand how activity routed through thalamus recombines with activity sent cortico-cortically. In the feedforward direction, current studies in our lab are exploring the effects of silencing S1 layer 5 terminals in POm on sensory discrimination and calcium activity in S2 cortex (and similarly silencing V1 layer 5 terminals in Pul). It could be the case, for example, that driving inputs from POm → S2 synapse onto separate cells that those receiving strong input from S1, driving separate populations, or it could be that these inputs sum their activity in S2 by synapsing onto the same cells. In this latter case, the spatial and temporal limits of that summation would be informative, since as mentioned earlier, transthalamic routes can be gated by inhibitory thalamic networks. In such a case, zona incerta and the thalamic reticular nucleus would be able to allow or disallow this summation.

Finally, *how general is the pattern that feedforward transthalamic pathways operate in a driver capacity, and feedback, in a modulatory one?* We mentioned this question briefly toward the end of Chapter 2, but will expand here since it is one of the main conclusions of this project. Our data suggest a pattern where feedforward transthalamic routes appear to drive targets in S2 and HVAs, and feedback transthalamic pathways modulate activity in S1 and V1. It is tempting to imagine that this pattern could generalize to other transthalamic circuitry, but that idea remains to be supported by real evidence. In part, it recalls a possible feature of cortico-cortical communication, where it has often been implied that feedforward pathways are made of robust (some even use the language, “driver”) synapses, while feedback must be modulatory. There are

good reasons for these assumptions in many cases, such as the relationship between the receptive field properties of a pre- and post-synaptic pair (one might expect them to be closely related if a connection were a driver, but not necessarily if that connection were a modulator), or the spatial extent of axonal arborizations (it seems logical that if an axon spans a large area where post-synaptic cells have different receptive fields, the axon must not be conveying basic receptive field information). But data directly supporting this assumption are scarce. As mentioned briefly in Chapter 2, our lab has provided limited data from slice physiology studies suggesting a mixture of driver and modulator responses in the feedforward and feedback directions in the visual (De Pasquale & Sherman, 2011) and auditory cortices (Covic & Sherman, 2011). Therefore, while it seems intuitive that cortico-cortical projections may have functional differences in the feedback vs. feedforward direction, strong evidence of this has been difficult to come by.

In the transthalamic pathways explored here, the divergence between HO thalamocortical synapses in primary vs. higher areas was stark. It is worth noting that no modulator-type responses were recorded in S2 or HVAs in our study. If feedback is strictly modulatory, it might be expected that higher cortical areas exert some feedback onto S2 or HVAs such as LM. Whether the observed pattern is because they receive no feedback through thalamus or whether we missed evidence of such projections is not clear. It would be intriguing, however, if HO thalamus only modulated the activity of primary cortical areas. It could be the case that this feedback indirectly modulates intermediate cortical areas via the feedforward projections from primary to secondary areas carrying a pre-modulated signal. Such an arrangement might reduce the redundancy of projections and allow HO thalamic input to intermediate areas such as S2 and LM to have a simplified driver-only role.

However compelling such speculation may be, however, more experimental evidence will be required before the generalizable patterns of organization and circuit logic of transthalamic pathways can be recognized. Future results may be very informative in this regard, since there are likely many transthalamic pathways that have not even been described.

REFERENCES

Agmon, A., & Connors, B. W. (1991). Thalamocortical responses of mouse somatosensory (barrel) cortexin vitro. *Neuroscience*, *41*(2–3), 365–379.

Alexander, D., & Wright, J. (2006). The maximum range and timing of excitatory contextual modulation in monkey primary visual cortex. *Visual Neuroscience*, *23*, 721–728. https://doi.org/10.1017/S0952523806230049

Audette, N. J., Bernhard, S. M., Ray, A., Stewart, L. T., & Barth, A. L. (2019). Rapid Plasticity of Higher-Order Thalamocortical Inputs during Sensory Learning. *Neuron*, *103*(2), 277-291.e4. https://doi.org/10.1016/j.neuron.2019.04.037

Bender, D. B. (1983). Visual activation of neurons in the primate pulvinar depends on cortex but not colliculus. *Brain Research*, *279*(1), 258–261. https://doi.org/10.1016/0006-8993(83)90188-9

Bickford, M. (2016). Thalamic Circuit Diversity: Modulation of the Driver/Modulator Framework. *Frontiers in Neural Circuits*, *9*, 86. https://doi.org/10.3389/fncir.2015.00086

Blot, A., Roth, M. M., Gasler, I., Javadzadeh, M., Imhof, F., & Hofer, S. B. (2021). Visual intracortical and transthalamic pathways carry distinct information to cortical areas. *Neuron*, *109*(12), 1996-2008.e6. https://doi.org/10.1016/j.neuron.2021.04.017

Brecht, M., Roth, A., & Sakmann, B. (2003). Dynamic receptive fields of reconstructed pyramidal cells in layers 3 and 2 of rat somatosensory barrel cortex. *The Journal of Physiology*, *553*(Pt 1), 243–265. https://doi.org/10.1113/jphysiol.2003.044222

Brumberg, J. C., Pinto, D. J., & Simons, D. J. (1999). Cortical Columnar Processing in the Rat Whisker-to-Barrel System. *Journal of Neurophysiology*, *82*(4), 1808–1817. https://doi.org/10.1152/jn.1999.82.4.1808

Callaway, E. M. (2004). Feedforward, feedback and inhibitory connections in primate visual cortex. *Neural Networks*, *17*(5), 625–632. https://doi.org/10.1016/j.neunet.2004.04.004

Callaway, E. M., & Luo, L. (2015). Monosynaptic circuit tracing with glycoprotein-deleted rabies viruses. *Journal of Neuroscience*, *35*(24), 8979–8985.

Constantinople, C. M., & Bruno, R. M. (2011). Effects and mechanisms of wakefulness on local cortical networks. *Neuron*, *69*(6), 1061–1068. https://doi.org/10.1016/j.neuron.2011.02.040

Covic, E. N., & Sherman, S. M. (2011). Synaptic properties of connections between the primary and secondary auditory cortices in mice. *Cerebral Cortex*, *21*(11), 2425–2441.

Crick, F., & Koch, C. (1998). Constraints on cortical and thalamic projections: The no-strong-loops hypothesis. *Nature*, *391*(6664), 245–250. https://doi.org/10.1038/34584

De Pasquale, R., & Sherman, S. M. (2011). Synaptic properties of corticocortical connections between the primary and secondary visual cortical areas in the mouse. *Journal of Neuroscience*, *31*(46), 16494–16506.

de Souza, B. O. F., Cortes, N., & Casanova, C. (2020). Pulvinar Modulates Contrast Responses in the Visual Cortex as a Function of Cortical Hierarchy. *Cerebral Cortex*, *30*(3), 1068–1086. https://doi.org/10.1093/cercor/bhz149

Diamond, M. E., Armstrong-James, M., & Ebner, F. F. (1992). Somatic sensory responses in the rostral sector of the posterior group (POm) and in the ventral posterior medial nucleus (VPM) of the rat thalamus. *Journal of Comparative Neurology*, *318*(4), 462–476.

El-Boustani, S., Sermet, B. S., Foustoukos, G., Oram, T. B., Yizhar, O., & Petersen, C. C. H. (2020). Anatomically and functionally distinct thalamocortical inputs to primary and

secondary mouse whisker somatosensory cortices. *Nature Communications*, *11*(1), 3342. https://doi.org/10.1038/s41467-020-17087-7

Fang, Q., Chou, X., Peng, B., Zhong, W., Zhang, L. I., & Tao, H. W. (2020). A Differential Circuit via Retino-Colliculo-Pulvinar Pathway Enhances Feature Selectivity in Visual Cortex through Surround Suppression. *Neuron*, *105*(2), 355-369.e6. https://doi.org/10.1016/j.neuron.2019.10.027

Groh, A., Bokor, H., Mease, R. A., Plattner, V. M., Hangya, B., Stroh, A., Deschenes, M., & Acsády, L. (2014). Convergence of Cortical and Sensory Driver Inputs on Single Thalamocortical Cells. *Cerebral Cortex*, *24*(12), 3167–3179. https://doi.org/10.1093/cercor/bht173

Guo, K., Yamawaki, N., Barrett, J. M., Tapies, M., & Shepherd, G. M. (2020). Cortico-thalamo-cortical circuits of mouse forelimb S1 are organized primarily as recurrent loops. *Journal of Neuroscience*, *40*(14), 2849–2858.

Hirsch, J. A., & Martinez, L. M. (2006). Laminar processing in the visual cortical column. *Current Opinion in Neurobiology*, *16*(4), 377–384. https://doi.org/10.1016/j.conb.2006.06.014

Hooks, B. M. (2017). Sensorimotor convergence in circuitry of the motor cortex. *The Neuroscientist*, *23*(3), 251–263.

Jackman, S. L., Beneduce, B. M., Drew, I. R., & Regehr, W. G. (2014). Achieving high-frequency optical control of synaptic transmission. *Journal of Neuroscience*, *34*(22), 7704–7714.

Jones, E. G. (2007). *The thalamus* (2nd ed). Cambridge University Press.

Jones, L. M., Fontanini, A., Sadacca, B. F., Miller, P., & Katz, D. B. (2007). Natural stimuli evoke dynamic sequences of states in sensory cortical ensembles. *Proceedings of the National Academy of Sciences*, *104*(47), 18772–18777. https://doi.org/10.1073/pnas.0705546104

Juavinett, A. L., Kim, E. J., Collins, H. C., & Callaway, E. M. (2020). A systematic topographical relationship between mouse lateral posterior thalamic neurons and their visual cortical projection targets. *Journal of Comparative Neurology*, *528*(1), 99–111.

Kennedy, H., & Bullier, J. (1985). A double-labeling investigation of the afferent connectivity to cortical areas V1 and V2 of the macaque monkey. *Journal of Neuroscience*, *5*(10), 2815–2830. https://doi.org/10.1523/JNEUROSCI.05-10-02815.1985

Kirchgessner, M. A., Franklin, A. D., & Callaway, E. M. (2021). Distinct "driving" versus "modulatory" influences of different visual corticothalamic pathways. *Current Biology*, *31*(23), 5121-5137.e7. https://doi.org/10.1016/j.cub.2021.09.025

Lee, C., & Sherman, S. (2009). Modulator property of the intrinsic cortical projection from layer 6 to layer 4. *Frontiers in Systems Neuroscience*, *3*. https://www.frontiersin.org/article/10.3389/neuro.06.003.2009

MacLean, J. N., Fenstermaker, V., Watson, B. O., & Yuste, R. (2006). A visual thalamocortical slice. *Nature Methods*, *3*(2), 129–134. https://doi.org/10.1038/nmeth849

Martinez, L. M., Wang, Q., Reid, R. C., Pillai, C., Alonso, J.-M., Sommer, F. T., & Hirsch, J. A. (2005). Receptive field structure varies with layer in the primary visual cortex. *Nature Neuroscience*, *8*(3), 372–379. https://doi.org/10.1038/nn1404

Masri, R., Bezdudnaya, T., Trageser, J. C., & Keller, A. (2008). Encoding of Stimulus Frequency and Sensor Motion in the Posterior Medial Thalamic Nucleus. *Journal of Neurophysiology*, *100*(2), 681–689. https://doi.org/10.1152/jn.01322.2007

Mease, R. A., Metz, M., & Groh, A. (2016). Cortical Sensory Responses Are Enhanced by the Higher-Order Thalamus. *Cell Reports*, *14*(2), 208–215. https://doi.org/10.1016/j.celrep.2015.12.026

Mo, C., Petrof, I., Viaene, A. N., & Sherman, S. M. (2017). Synaptic properties of the lemniscal and paralemniscal pathways to the mouse somatosensory thalamus. *Proceedings of the National Academy of Sciences*, *114*(30), E6212–E6221.

Mo, C., & Sherman, S. M. (2019). A sensorimotor pathway via higher-order thalamus. *Journal of Neuroscience*, *39*(4), 692–704.

Murata, Y., & Colonnese, M. T. (2016). An excitatory cortical feedback loop gates retinal wave transmission in rodent thalamus. *ELife*, *5*, e18816. https://doi.org/10.7554/eLife.18816

Nakajima, M., & Halassa, M. M. (2017). Thalamic control of functional cortical connectivity. *Current Opinion in Neurobiology*, *44*, 127–131.

Nakamura, H., Hioki, H., Furuta, T., & Kaneko, T. (2015). Different cortical projections from three subdivisions of the rat lateral posterior thalamic nucleus: A single-neuron tracing study with viral vectors. *European Journal of Neuroscience*, *41*(10), 1294–1310.

Ohno, S., Kuramoto, E., Furuta, T., Hioki, H., Tanaka, Y. R., Fujiyama, F., Sonomura, T., Uemura, M., Sugiyama, K., & Kaneko, T. (2012). A Morphological Analysis of Thalamocortical Axon Fibers of Rat Posterior Thalamic Nuclei: A Single Neuron Tracing Study with Viral Vectors. *Cerebral Cortex*, *22*(12), 2840–2857. https://doi.org/10.1093/cercor/bhr356

Pais-Vieira, M., Lebedev, M. A., Wiest, M. C., & Nicolelis, M. A. L. (2013). Simultaneous Top-down Modulation of the Primary Somatosensory Cortex and Thalamic Nuclei during Active Tactile Discrimination. *Journal of Neuroscience*, *33*(9), 4076–4093. https://doi.org/10.1523/JNEUROSCI.1659-12.2013

Payne, B. R. (1993). Evidence for Visual Cortical Area Homologs in Cat and Macaque Monkey. *Cerebral Cortex*, *3*(1), 1–25. https://doi.org/10.1093/cercor/3.1.1

Petrof, I., Viaene, A. N., & Sherman, S. M. (2015). Properties of the primary somatosensory cortex projection to the primary motor cortex in the mouse. *Journal of Neurophysiology*, *113*(7), 2400–2407.

Petty, G. H., Kinnischtzke, A. K., Hong, Y. K., & Bruno, R. M. (2021). Effects of arousal and movement on secondary somatosensory and visual thalamus. *ELife*, *10*, e67611. https://doi.org/10.7554/eLife.67611

Purushothaman, G., Marion, R., Li, K., & Casagrande, V. A. (2012). Gating and control of primary visual cortex by pulvinar. *Nature Neuroscience*, *15*(6), 905–912. https://doi.org/10.1038/nn.3106

Rafal, R. D., & Posner, M. I. (1987). Deficits in human visual spatial attention following thalamic lesions. *Proceedings of the National Academy of Sciences*, *84*(20), 7349–7353. https://doi.org/10.1073/pnas.84.20.7349

Reichova, I., & Sherman, S. M. (2004). Somatosensory corticothalamic projections: Distinguishing drivers from modulators. *Journal of Neurophysiology*, *92*(4), 2185–2197.

Reinhold, K., Lien, A. D., & Scanziani, M. (2015). Distinct recurrent versus afferent dynamics in cortical visual processing. *Nature Neuroscience*, *18*(12), 1789–1797. https://doi.org/10.1038/nn.4153

Richard, D., Gioanni, Y., Kitsikis, A., & Buser, P. (1975). A study of geniculate unit activity during cryogenic blockade of the primary visual cortex in the cat. *Experimental Brain Research*, *22*(3), 235–242. https://doi.org/10.1007/BF00234766

Rockland, K. S. (2019). Distinctive Spatial and Laminar Organization of Single Axons from Lateral Pulvinar in the Macaque. *Vision*, *4*(1), 1. https://doi.org/10.3390/vision4010001

Rockland, K. S., Andresen, J., Cowie, R. J., & Robinson, D. L. (1999). Single axon analysis of pulvinocortical connections to several visual areas in the Macaque. *Journal of Comparative Neurology*, *406*(2), 221–250. https://doi.org/10.1002/(SICI)1096-9861(19990405)406:2<221::AID-CNE7>3.0.CO;2-K

Rodriguez-Moreno, J., Porrero, C., Rollenhagen, A., Rubio-Teves, M., Casas-Torremocha, D., Alonso-Nanclares, L., Yakoubi, R., Santuy, A., Merchan-Pérez, A., DeFelipe, J., Lübke, J. H. R., & Clasca, F. (2020). Area-Specific Synapse Structure in Branched Posterior Nucleus Axons Reveals a New Level of Complexity in Thalamocortical Networks. *Journal of Neuroscience*, *40*(13), 2663–2679. https://doi.org/10.1523/JNEUROSCI.2886-19.2020

Roth, M. M., Dahmen, J. C., Muir, D. R., Imhof, F., Martini, F. J., & Hofer, S. B. (2016). Thalamic nuclei convey diverse contextual information to layer 1 of visual cortex. *Nature Neuroscience*, *19*(2), 299–307. https://doi.org/10.1038/nn.4197

Saalmann, Y. B., & Kastner, S. (2015). The cognitive thalamus. *Frontiers in Systems Neuroscience*, *9*, 39. https://doi.org/10.3389/fnsys.2015.00039

Saalmann, Y. B., Pinsk, M. A., Wang, L., Li, X., & Kastner, S. (2012). The pulvinar regulates information transmission between cortical areas based on attention demands. *Science*, *337*(6095), 753–756.

Sampathkumar, V., Miller-Hansen, A., Murray Sherman, S., & Kasthuri, N. (2021). An ultrastructural connectomic analysis of a higher-order thalamocortical circuit in the mouse. *European Journal of Neuroscience*, *53*(3), 750–762.

Sampathkumar, V., Miller-Hansen, A., Sherman, S. M., & Kasthuri, N. (2021). Integration of signals from different cortical areas in higher order thalamic neurons. *Proceedings of the National Academy of Sciences*, *118*(30).

Scala, F., Kobak, D., Shan, S., Bernaerts, Y., Laturnus, S., Cadwell, C. R., Hartmanis, L., Froudarakis, E., Castro, J. R., Tan, Z. H., Papadopoulos, S., Patel, S. S., Sandberg, R., Berens, P., Jiang, X., & Tolias, A. S. (2019). Layer 4 of mouse neocortex differs in cell types and circuit organization between sensory areas. *Nature Communications*, *10*(1), 4174. https://doi.org/10.1038/s41467-019-12058-z

Schwarz, L. A., Miyamichi, K., Gao, X. J., Beier, K. T., Weissbourd, B., DeLoach, K. E., Ren, J., Ibanes, S., Malenka, R. C., Kremer, E. J., & Luo, L. (2015). Viral-genetic tracing of the input–output organization of a central noradrenaline circuit. *Nature*, *524*(7563), 88–92. https://doi.org/10.1038/nature14600

Shadlen, M. N., & Newsome, W. T. (1994). Noise, neural codes and cortical organization. *Current Opinion in Neurobiology*, *4*(4), 569–579. https://doi.org/10.1016/0959-4388(94)90059-0

Sherman, S. M. (2016). Thalamus plays a central role in ongoing cortical functioning. *Nature Neuroscience*, *19*(4), 533–541.

Sherman, S. M., & Guillery, R. W. (1998). On the actions that one nerve cell can have on another: Distinguishing "drivers" from "modulators." *Proceedings of the National Academy of Sciences*, *95*(12), 7121–7126.

Sherman, S. M., & Guillery, R. W. (2013). *Functional Connections of Cortical Areas: A New View from the Thalamus*. MIT Press.

Sherman, S. M., & Usrey, W. M. (2021). *Exploring Thalamocortical Interactions: Circuitry for Sensation, Action, and Cognition*. Oxford University Press.

Shumkova, V., Sitdikova, V., Rechapov, I., Leukhin, A., & Minlebaev, M. (2021). Effects of urethane and isoflurane on the sensory evoked response and local blood flow in the early postnatal rat somatosensory cortex. *Scientific Reports*, *11*(1), 9567. https://doi.org/10.1038/s41598-021-88461-8

Siegle, J. H., Jia, X., Durand, S., Gale, S., Bennett, C., Graddis, N., Heller, G., Ramirez, T. K., Choi, H., Luviano, J. A., Groblewski, P. A., Ahmed, R., Arkhipov, A., Bernard, A., Billeh, Y. N., Brown, D., Buice, M. A., Cain, N., Caldejon, S., … Koch, C. (2021). Survey of spiking in the mouse visual system reveals functional hierarchy. *Nature*, *592*(7852), 86–92. https://doi.org/10.1038/s41586-020-03171-x

Snow, J. C., Allen, H. A., Rafal, R. D., & Humphreys, G. W. (2009). Impaired attentional selection following lesions to human pulvinar: Evidence for homology between human and monkey. *Proceedings of the National Academy of Sciences*, *106*(10), 4054–4059. https://doi.org/10.1073/pnas.0810086106

Theyel, B. B., Llano, D. A., & Sherman, S. M. (2010). The corticothalamocortical circuit drives higher-order cortex in the mouse. *Nature Neuroscience*, *13*(1), 84–88. https://doi.org/10.1038/nn.2449

Thomson, A. M. (2000). Facilitation, augmentation and potentiation at central synapses. *Trends in Neurosciences*, *23*(7), 305–312. https://doi.org/10.1016/S0166-2236(00)01580-0

Urbain, N., Salin, P. A., Libourel, P.-A., Comte, J.-C., Gentet, L. J., & Petersen, C. C. H. (2015). Whisking-Related Changes in Neuronal Firing and Membrane Potential Dynamics in the Somatosensory Thalamus of Awake Mice. *Cell Reports*, *13*(4), 647–656. https://doi.org/10.1016/j.celrep.2015.09.029

Van Essen, D. C., & Maunsell, J. H. R. (1983). Hierarchical organization and functional streams in the visual cortex. *Trends in Neurosciences*, *6*, 370–375. https://doi.org/10.1016/0166-2236(83)90167-4

Veinante, P., Jacquin, M. F., & Deschênes, M. (2000). Thalamic projections from the whisker-sensitive regions of the spinal trigeminal complex in the rat. *Journal of Comparative Neurology*, *420*(2), 233–243.

Viaene, A. N., Petrof, I., & Sherman, S. M. (2011a). Properties of the thalamic projection from the posterior medial nucleus to primary and secondary somatosensory cortices in the mouse. *Proceedings of the National Academy of Sciences*, *108*(44), 18156–18161.

Viaene, A. N., Petrof, I., & Sherman, S. M. (2011b). Synaptic properties of thalamic input to layers 2/3 and 4 of primary somatosensory and auditory cortices. *Journal of Neurophysiology*, *105*(1), 279–292.

Viaene, A. N., Petrof, I., & Sherman, S. M. (2013). Activation requirements for metabotropic glutamate receptors. *Neuroscience Letters*, *541*, 67–72. https://doi.org/10.1016/j.neulet.2013.02.004

Wang, Q., Gao, E., & Burkhalter, A. (2011). Gateways of ventral and dorsal streams in mouse visual cortex. *Journal of Neuroscience*, *31*(5), 1905–1918.

Ward, R., Danziger, S., Owen, V., & Rafal, R. (2002). Deficits in spatial coding and feature binding following damage to spatiotopic maps in the human pulvinar. *Nature Neuroscience*, *5*(2), 99–100. https://doi.org/10.1038/nn794

Yang, T., & Maunsell, J. H. R. (2004). The Effect of Perceptual Learning on Neuronal Responses in Monkey Visual Area V4. *Journal of Neuroscience*, *24*(7), 1617–1626. https://doi.org/10.1523/JNEUROSCI.4442-03.2004

Zhang, W., & Bruno, R. M. (2019). High-order thalamic inputs to primary somatosensory cortex are stronger and longer lasting than cortical inputs. *ELife*, *8*, e44158. https://doi.org/10.7554/eLife.44158

Zhou, N. A., Maire, P. S., Masterson, S. P., & Bickford, M. E. (2017). The mouse pulvinar nucleus: Organization of the tectorecipient zones. *Visual Neuroscience*, *34*.

Zipser, K., Lamme, V. A. F., & Schiller, P. H. (1996). Contextual Modulation in Primary Visual Cortex. *The Journal of Neuroscience*, *16*(22), 7376–7389. https://doi.org/10.1523/JNEUROSCI.16-22-07376.1996